3D creep cavitation characteristics and residual life assessment in high temperature steels: a critical review

Gupta, C
Mechanical Metallurgy Division, Materials Group, Bhabha AtomicResearch Centre, Mumbai

Toda, Hiroyuki
Toyohashi University of Technology

Mayi, P.
Institute of Joining and Assembly, Chemnitz University of Technology

Sommitsch, C.
Institute for Materials Science and Welding, Graz University of Technology

出版情報：Materials Science and Technology. 31, pp.603-626, 2014-10-22. Institute of Metals
バージョン：
権利関係：

For special issue on "*Cavitation : New Insights….*" in MST

3D creep cavitation characteristics and residual life assessment in steels: Critical review

C. Gupta[1#], H. Toda[2], P. Mayr[3], C. Sommitsch[4]

1. Mechanical Metallurgy Division, Materials Group, Bhabha AtomicResearch Centre, Mumbai - 400085, India
2. Department of Mechanical Engineering, Kyushu University, Nishi-Ku, Fukuoka 819-0359, Japan.
3.Institute of Joining and Assembly, Chemnitz University of Technology, Reichenhainerstraβe 70, 09126 Chemnitz Germany.
4.Institute for Materials Science and Welding, Graz University of Technology, Kopernikussgasse 24/l-A 8010, Graz, Austria.
#: Former JSPS fellow and visiting Associate Professor at Department of Mechanical Engineering Toyohashi University of Technology, Toyohashi, Aichi, Japan.

Abstract

The paper seeks to assess critically the need for a new paradigm in creep life estimation of service exposed steels and provide possible new directions of residual life assessment, in the light of a decade of explosive application of micro-tomography on structural materials to characterise the 3D nature of cavitation damage. The phenomenon of creep failure using synchrotron micro-tomography (SR-μCT) has been studied at large synchrotron sources where imaging on conventional structural materials such as steels with high absorption to X-rays has been realized. The unique feature of the SR-μCT studies is the direct imaging in 3D of cavitation present in the bulk (hundreds of micrometers in size), revealing the spatial characteristics and morphology of the creep voids. Further the quantitative analyses of cavitation characteristics contained in the 3D datasets, which when scaled with time, stress and temperature provides functional information amenable for developing constitutive equations for creep fracture. These being based on SR-μCT, which due to its non-destructive feature provides high fidelity data that significantly reduces the ambiguity in the development of the functional relationships related to creep failure. Thus the use of such constitutive equations in an explicit manner to estimate the residual life of the components affected by creep and the consequent assessment of structural integrity would prove invaluable. This paper summarizes the studies related to creep in materials using micro-tomography with special emphasis on a 10.86%Cr heat resistant steel to show the type of data available which could be relevant for life assessment and design against creep failure. A brief discussion of the existing methods of residual life estimations in the light of the availability of the 3D micro-tomography data available in recent literature follows. Finally the possible new directions of using the micro-tomography data to formulate advanced residual life estimation methods are briefly touched.

Introduction

The creep phenomenon in structural materials has received intensive interest due to its ubiquitous presence in high temperature components of power plants[1-3]. It is realized that creep failure in structural materials for high temperature application such as steels cannot be

eliminated but only delayed. Thus, the benefit derived from creep research basically translates into extending the life of components with use of newer heat resistant materials with enhanced inherent creep resistance beyond the economic operation period of the power plants. Creep resistance in structural materials could be achieved by controlling two broad factors – increasing the thermal stability of microstructure and providing for a crept microstructure that is tolerant to damage by cavitation and cracking[4-9]. Over the past four decades great strides have been made in understanding the factors contributing to high temperature microstructural stability of various classes of materials[10,11]. This is particularly true for tempered martensitic steels, where the 100 MPa - 10^5 hour creep life has been progressively increased from 400°C to 650°C. Figure 1 depicts the stress – rupture life relationship for various 9-12%Cr heat resistant steels showing that the 100 MPa - 10^5 hour creep life for the more modern variants is in the range 500-650°C. These experiences have emboldened compositional developments to further improve the inherent creep failure resistance of tempered martensitic steels, notably being illustrated by the recent efforts to modify P92 compositions with B and N[12-14]. Thus the application of metallurgical design has resulted in the development of tempered martensitic alloys with enhanced microstructural stability at elevated temperatures[15].

The research on the development of damage in materials, in this case via creep cavitation is particularly characterized by a lack of clarity[16] as compared to those concerning microstructural stability of heat resistant steels. There is general acceptance on the effects that a present creep damage would cause on the macroscopic properties. In the case of creep the onset of significant cavitation damage has been recognized to result in an increase of the creep rate[17]. Using techniques such as surface replication the evolution of creep cavitation in steels has been classified into four stages namely isolated cavities, orientated cavities, linked cavities and macrocracks[18]. This evolution of the stages of cavitation is shown in figure 2 schematically. However, the understanding of the way in which damage proliferates within the bulk due to degradation phenomena such as creep is still not clear. This lack of understanding is mainly due to the unavailability of suitable techniques to characterize the presence of damage in materials. Optical microscopy and electron microscopy techniques have been the mainstay of these traditional techniques to characterize damage. While these techniques, especially the electron microscopy ones have been developed significantly to characterize the elevated temperature microstructures of tempered martensitic steels at nano-length scales (even providing for in-situ experiments as illustratively shown in a study reported on 12Cr-2W-5Co steel at 650°C[19,20] by Blum[21]) , their suitability to characterize damage, i.e. voids and cracks is

poor. Due to the destructive sample preparation techniques for microscopy characterization many of the finer sized pores and cracks are polished out and are eclipsed from observation. Further, the characterization takes place in 2D, where the true shape and size of the pores and cracks cannot be revealed. A non-destructive technique that provides 3D visualization the damage would be much more suitable for studying its nature.

The tomography technique that provides a non-destructive image in 3D has emerged as the most suitable tool to study damage in materials[22]. The turn of the 21st century saw the successful operation of the large synchrotron radiation facilities such as SPring-8, ESRF and APS[23]. High fidelity reconstructed 3D images of the bulk containing damage in materials due to processing conditions (such as casting, forming and heat treatment) as well as multifarious failures of service exposed components could be routinely available at these large synchrotron sources by application of the micro-tomography technique[24]. While the 3D imaging and visualization of the tomography datasets provides information on the true morphology of the various types of damage occurring due to degradation phenomena, a number of new techniques based on micro-tomography technique have been developed that provides a mechanistic insight on the interaction of microstructure with the proliferation of the micro-damage[25]. These new investigative methods include the analysis of the 3D nature of grain structures, second phases, as well as the local distribution of damage and strain. Thus the application of the micro-tomography technique at large synchrotron sources has provided a new paradigm in the understanding of the mechanical behavior of materials within the traditional framework of structure – property correlation with the explicit inclusion of damage structure and its interaction with the causative microstructural entities in the micron length scale.

The implications of these techniques and the resulting scientific studies in understanding the development of damage in structural materials, on the methods to assess the residual life and structural integrity are quite significant. The importance of tomographic techniques for structural integrity and performance of engineering materials was pioneered at ESRF (Beam line ID19) where combined SR-μCT and synchrotron diffraction experiments were carried out to image growth of fatigue cracks. In these experiments, additionally, crack tip strains could be measured and post-experiment numerical computation of stresses was able to validate models used for fatigue life prediction[26]. As already pointed out a tenuous understanding of the underlying mechanisms of damage propagation and its implication on failure exists. Despite this a variety of schemes for residual life assessment and structural integrity methods have been developed[27]. In the context of creep the development of 3D techniques now enable a conception

of the life assessment on the basis of functional relationships between internal damage and macroscopic quantities such as stress, strain and temperature. The constitutive relationships for creep that enable life prediction can be developed considering the characteristics of micro-damage such as number density, volume fraction, growth rate etc. determined from micro-tomography experiments. In this paper these new approaches on developing advanced residual life estimations on the basis of physically relevant tomographic data on creep cavitation characteristics are explored by taking the case of a 10.86%Cr heat resistant steel. The tomography characterization of the steel has been carried out at SPring-8, the world's largest synchrotron source on sample coupons extracted from specimens crept at 600°C over the stress range 120 – 180 MPa[28]. The paper will first present a summary of a selected set of research characterizing cavitation in materials using 3D/4D methods; followed by a critical review of the existing measures of estimating creep life used in heat resistant steel; and then by the presentation of the tomographic results obtained in CB8 steel (showing transition from transgranular to intergranular fracture over the stress range 120 – 180 MPa), E911 & P91 steel in multi-axial long term creep and Type IV failure in MARBN steel weldments. Finally new directions and possibilities to develop advanced residual life estimations of heat resistant steels will be elucidated.

2. Multi-modal and Multi-scale characterisation of Cavitation in Engineering Materials

The section concerns with providing a summary of the typical application of a variety of 3D/4D techniques for research into cavitation led failure (including creep) of engineering materials. In the scheme of the present review on the implications that the extensive application of micro-tomography on materials has had on the methods and techniques of residual life estimation of component, the section seeks to illustrate the range of information typically available from application of latest 3D/4D techniques so that a critical discussion on the end of life criteria can be presented in the following sections. Exhaustive reviews on the principles and applications of the tomography technique on failure mechanisms of materials have been published by Stock[22,23], which this section does not attempt to do.

The development of damage in materials that play a key role in failure of engineering materials depend on a multitude of factors. It is therefore useful to not only chronologically map their evolution from the incipient stages but also provide means to relate their development to the evolving microstructure. Thus in order to fully understand the role played by damage to cause failure a multi-modal and multi-scale characterisation is required. The application of

synchrotron micro-tomography has provided new insights for various failure mechanisms in materials[22-25,29,30]. This has been primarily possible by revealing the interplay between the development of cavitation in materials and microstructural features such as particles and grain boundaries. Deeper insights have been facilitated by advances in 3D imaging and the development of analysis techniques such as high resolution 3D imaging, phase contrast imaging, strain mapping, chemical mapping in 3D, local driving force mapping in cracked bodies etc. Several reviews have been devoted to summarise the literature relating to advanced analysis using micro-tomography technique[22,23,25]. For example in one of the early studies Buffiere et al.[31] mapped the evolution of damage in Al based metal matrix composites in in-situ experiments. The sample dimension for the in-situ studies was 1.5 x 1.5 x 4 mm^3 and reconstructions were carried out using isotropic voxel size of 6.65μm. These investigations revealed the importance of the matrix strength in metal matrix composites to decisively influence the mechanism of fracture in case of aluminium alloy – zirconia/silica composites. While damage in the low strength matrix was at the particle – matrix interface, the higher strength matrix showed particle cracking. The issue of crack closure was one of the first problems to be investigated using micro-tomography as it permitted the 3D visualisation of the faces of the crack at different points in the fatigue cycle. The well known Roughness induced crack closure (RICC) of cracks that propagate in ductile metals such as aluminium alloys reduces the applied stress intensity and leads to an "artificial" lowering of crack growth rates. 3D visualisation of the abutting crack faces reveals the physical origins of the RICC. Guvenilir, Stock and others[32-34], showed in an aluminium alloy AA2090 T841 that the crack front was not uniformly rough behind its tip which resulted in a mixed mode contact of the crack faces. While the planar sections were closed at a much greater closure load level, the rough areas progressively underwent closure with load resulting in progressive stiffening of the sample. Subsequent investigations using high resolution tomography by Toda et al.[35] were able to not only confirm these trends but also to measure the crack tip displacements during the process of closure using the micro-voids as fiducial markers. The closure behaviour was found to be significantly influenced by the mode III displacements that were associated with the local crack topology and was sustained near to the maximum load in the cycle. The use of the concept of tracking fiducial markers composed of the cavitation artefacts such as micro-voids was extended to particle tracking in successive micro-tomography datasets obtained by in-situ experiments by Nielsen et al.[36,37] and Kobayashi et al[38]. These were used to develop an important analysis tool to carry out high density strain mapping on a local scale that could

reveal mechanisms of deformation and damage processes in various structural materials such as foams, light metal alloys and steels.

The phenomenon of creep cavitation in materials has also been investigated using synchrotron X-ray micro-tomography[39-49]. In one of the first studies employing short term in-situ creep in pre-deformed brass (Cu-40Zn-2Pb) tested at 375°C and 25 MPa, the evolution of cavitation characteristics in terms of pore size and volume were mapped through a creep exposure time of just over 7 hours[39]. The sample size undergoing creep in these experiments was 1 mm in diameter and 2 mm in length. The reconstructions were carried out using an isotropic voxel size of 1.6μm. These experiments by Pyzalla et. al.[39] pioneered combining the "fast" tomography experiment with diffraction that provided information on the texture, internal stress distribution and dislocation density evolution during creep. Thus a relationship between cavitation damage and microstructural evolution was chronologically mapped. An exponential growth relationship was determined between the void volume computed from the quantitative analysis of the tomography dataset and creep time. The decrease in the reflection line profile analysis parameter was seen quite sharply with creep time until the saturation levels were attained, where the average void volume increased. At these creep times in the two phase brass the development of a fiber texture was detected using energy dispersive diffraction pattern analysis. Thus the appearance of large scale cavitation in the alpha-beta brass could be correlated with significant changes in the microstructure, i.e. a decrease in dislocation density and the appearance of local texturing. As these tests were carried out under a temperature gradient, an analysis was carried out by Sket et. al.[40], which monitored the dimensional changes of multiple local sub-volume regions in the tomographic sample dataset captured at periodic intervals within the creep exposure time to develop a procedure to compute the apparent activation energy for creep. The values of the activation energy correlated well with those obtained from conventional tests using larger samples. In-situ creep tests using synchrotron micro-tomography has also been carried out on Al MMC consisting of Al-11Zn-0.2Mg matrix containing 15%alumina short fibres[41]. From the creep tests carried out on suitably designed miniature samples, that were carefully established represent the behaviour seen in the larger standard samples, a new insight on development of damage was revealed by the tomographic imaging. The creep damage in Al MMC not only consisted of the cracking of the fibres, but additional void formation was discerned to be present within the fibre debris.

The progress of creep cavitation in materials is about nucleation, growth and coalescence of voids. Micro-tomography has been attempted for the direct observation of void growth and coalescence for ductile fracture phenomena in engineering materials. It has thus been possible to quantify the contributions from nucleation, growth and the coalescence process. This has however proved to be a non-trivial task both from the view point of technique development as well as subsequent analysis. Reasonable confidence in imaging the individual stages in the ductile damage required the development of the "continuous" tomography technique that proceeded to scan the sample without an interruption of the test. The required analysis tracks the change in morphology of thousands of voids to arrive at reasonable estimates of growth and coalescence. In case of creep the morphological changes proceed in a not so dramatic fashion as in ductile fracture, which lessens the burden to image their changes during the in-situ experiment. However, the ranges of the morphological changes are seen to be quite wide (especially when coalescence sets in), which necessitates the formulation of morphological indices that captures the multiplicity of changes in void shape, size and volume of the cavitating creep voids. In this regard Issac et. al.[42] developed a set of metrics to describe the complex morphological evolution of voids during creep. The power of the in-situ micro-tomography to provide new insights into the creep damage process was demonstrated by Diezciol et. al.[43] who carried out the measurement of void growth rate in copper and showed that the functional form of phenomenological growth laws assuming power law creep grossly underestimates the actual growth rates.

The recent developments in the application of micro-tomography to characterize damage in materials involve techniques of combining it with destructive 3D techniques. The advantages of these latter techniques that are mainly based on the serial sectioning principles, are to provide the characterization of microstructural elements such as grain boundaries and their orientations. These features, when incorporated in a dataset containing tomographic information on damage, provides multi-modality which can contain provide new mechanistic insights on the failure process in materials. In this regard Kral and co-workers[50,51] characterised the creep voids in an ex-service hydrogen reformer tube of austenitic stainless steel using serial sectioning over a small volume of 400µm x 300µm x 30-50µm. From a cross-section of the reformer tube exposed to varying temperature - stress condition from the inner to outer wall, serial sectioning carried out at four locations revealed significant difference in the creep void characteristics such as void count, volume and size distribution. Additional EBSD scans at regular intervals gave the miss-orientation information of the grains across the section of the tube containing

fine equi-axed structure at inner wall to large columnar ones at the outer wall . Thus the varying grain characteristic from a size of ~450μm at outer wall to 50μm at inner wall was shown to correlate with the void densities at the grain boundaries. Further the grain miss-orientation in the range 50° - 70° was found to contain greater voids. Asghar, Requena and co-workers[44,45] have studied a series of Al-Si eutectic cast alloys with Ni, Cu additions and a spheroidising treatment for improving the high temperature creep properties for piston applications. The long range 3D network of the Si in an α-Al matrix strengthened by the presence of primary aluminides were found to be beneficial for the high temperature properties. The use of serial sectioning using optical microscopy and synchrotron micro-tomography in a complementary way, was able to reveal the interconnectivity and contiguity between Si and aluminides in 3D. Recently Yazzie et. al.[46] combined synchrotron X-ray micro-tomography and FIB-SEM to provide a multi-scale characterisation of the precipitates in Sn-Ag, Sn-Cu and Sn-Pb solder joints. Thus the resolution range of the characterization was increased from micro-meter to sub-micrometer level. The complementary use of the techniques was able to characterise the nano-scale Ag_3Sn precipitates in the Sn-rich dendrites observed in tomography dataset. However these studies do not provide a multimodal dataset of serial sectioning and tomography.

The brief summary presented above based on typical studies aimed at revealing the mechanisms of failure in selected engineering materials highlights the emergence of destructive 3D techniques along with the advances in tomographic evaluation of damage. This is because these techniques provide micro-structural information that is quite valuable for a mechanistic interpretation of the failure. In this regard the use of FIB-SEM instrument with automated features has emerged to obtain multi-modal information in 3D using serial sectioning by applying the cross-section ion milling technique (usually Ga^+ ion sputtering)[52] The nature of information characterised in 3D could be the general microstructural features such as precipitates, grains, and damage such voids as well as orientation of grain and chemical mapping of elements. The imaging of the fine micro-structural features in the nano-meter scale visualised in 3D using voxel dimensions in tens of nano-meters can be characterised over typical volumes of about 1000 um^3 using FIB-SEM. In contrast the imaging capability of high resolution tomography using Fresnel zone plates can go down to only about 200 nm in dense structural materials such as aluminium[53]. However, the advantages of resolution and multi-modality capability of the destructive 3D characterisation technique pale in comparison to the versatility of the tomographic technique as an investigative tool to be adapted to conduct in-situ experiments that provides real time 4D dataset containing chronological mapping of

damage, grain and even local strain as a function of applied stress and strain. In case of long term creep of materials, however, the relevance of in-situ experimentation is of little value in revealing the mechanisms of damage. Despite the advantages of the destructive 3D techniques the relevance of the non-destructive imaging techniques for ex-situ imaging is quite germane considering the speed in obtaining a high fidelity 3D dataset at large synchrotron sources such as SPring-8 and ESRF, where the true morphology of the internal structure such as damage and second phases are revealed. The reconstructed 3D dataset at these beamlines at large synchrotron sources are based on superimposed image contrast due to absorption and phase changes of the incident X-ray beam which not only enhances the resolution metrics but also provides greater confidence to assess the true 3D nature of the imaged micro-structural features. In contrast the serial sectioning method to generate a 3D dataset presents a challenge to obtain the slices in their original form unscathed from the sputtering process[52]. Therefore careful optimisation of sputtering parameters to minimise material damage and its maintenance of these parameters over the long times (in the range of days) are quite critical to the success of the FIB-SEM to provide high – fidelity 3D dataset. Thus typically work-flow automation for obtaining the 2D image slice stack is the norm so that repeatable results are obtained. Further, the large volume of data obtained for a given region needs to be post processed for registration of the finely spaced slices and segmentation of the objects contained in them in an automated manner. All these are steps are carried out using automated mode.

The selected presentation of tomographic investigations in different materials summarised above therefore yields information in the micro-meter length scale on the 3D characteristics of damage contained in materials. These characteristics could be determined either in an ex-situ manner or using in-situ experiments. The 3D characteristics that are determined could be either overall parameters such as volume fraction, number density, size distribution or individual parameters such as void shape, complexity or its spatial distribution. These 3D characteristics of damage are constrained to be determined by a volume of scan that depends on the resolution desired and density of materials. At the limit of the resolution in the micro-meter scale at large synchrotron sources (~ 1µm; eg BL20XU, SPring-8) the typical volume in a single scan is about 600 micro-meter cube in steels and aluminium alloys. For heat resistant steels this volume of scan typically encompasses equivalent to 5000 – 25000 spherical shaped grains of size 30 – 50 µm. In such volumes large number of damage in terms of voids can be detected, ensuring the statistical robustness of the quantitative analysis of the 3D dataset. In long term creep specimens however grain coarsening occurs, growing as in case of CB8 to about average

600µm after 6 years. In such a case the characterised volume may be increased by contiguous scanning of adjacent regions. In a coarsend microstructure it is useful to know the grain structure in 3D both for mechanistic interpretations and estimation of the grain volume that has been characterised. However, as absorption tomography is unable to image the microstructure such as grain use of techniques such as combining it with phase (eg holo-tomography) or diffraction (eg: diffraction contrast tomography) or serial sectioning have to be considered. On relaxing the resolution requirements the use of new generation lab based multi-scale tomographs may also be employed that can visualise non-destructively both large voids and their relation to cracks. Thus many possibilities exist to provide 3D characteristics of creep damage using the tomographic technique that can provide unambiguous end of life criteria for residual life estimation in an in-expensive manner.

3. **Measures of Estimating Creep Life in Steels : A critical review**

One of the earliest methods proposed to estimate creep life was the life fraction rule (LFR) by Robinson[54]. The rule in its generalized form can be mathematically represented as :

$$\sum \frac{\delta t_i(\sigma, T)}{t_i^r(\sigma, T)} = k \qquad (1)$$

Where $\delta t_r(\sigma, T)$ is the time spent at stress σ and temperature T; $t_i^r(\sigma, T)$is the rupture time at stress σ and temperature T and k is a constant, generally taken as unity.

The LFR postulates that a component exposed to a series of stress and temperature combinations, can be in use until the addition of the life fraction in each of the combination may reach the constant value k. This is generally taken as unity as per the original proposition by Robinson. But the constant was found to deviate from unity, in case of sequences of stress exposures (at constant temperature) to the material that are either monotonically increases or decreases in a step wise manner with time[55-57]. Such monotonic temperatures excursions however predicted a k value of ~ 1. Two underlying assumptions on this are that the material behaviour is history independent and the fact that the rupture life at specific combinations of stress and temperature was known. Although the LFR rule was very popular in the early days, its reliability to provide reasonable estimates failed due to the realization that the influences of factors such as material variability, lack adequate procedures for data extrapolation for the long term creep domain (> 30000 hours) and the increasing influence of environmental effects such as oxidation were non-trivial. An alternate method using area modified stresses has been

proposed by Hart[55] for the determination of residual life on using accelerated rupture tests on material exposed to creep damage in service. Rather than using the time fraction, the use of strain fraction as a measure of creep life assessment has also been proposed, bestowing the life evaluating parameter the consideration of a state variable[33]. This misplaced understanding that the creep strain fraction is dependent only on final values of stress and temperature and not on the character of their excursions has been clarified[58]. Furthermore critique of life / strain fraction rule to not consider the change in mechanisms of failure from ductile to inter-granular under stress-temperature combinations has also been pointed out[59]. Thus the applicability of the life fraction is limited to the cases where the stress temperature regime is such that creep mechanism does not change.

An alternative approach for appraisals of life assessment is based on the parameterisation of the creep curve in terms of strain – time[60-63] or strain rate – time[64,65] at various stress levels. From these predictive models constitutive equations have been developed to estimate the creep failure strains as a function of stress and temperature. These approaches, in contrast to the LFR method applicable to components, are focussed to predict the creep behaviour of the material itself. It is well known that creep regimes of a material, observed from tests, can be categorised into primary, secondary and tertiary stages. The widely used creep test data for a mathematical descriptions of the primary and tertiary stages using model equations is the strain – time plot over a given range of stresses. Typically these stages have been described by power and exponential equations. For example the primary and tertiary creep stages have been described by a power law equation by Graham and Walles[61] between strain and creep time in the following form :

$$\varepsilon = kt^{p} (2)$$

Where, the creep time (t) exponent p is 1/3 for the primary creep and 3 for the tertiary creep stage. The creep strain is represented as ε. Figure 3 shows typical creep strain – time curves of advanced 9 – 12% Cr heat resistant steel reported in recent literature[41-43]. The exponential nature of the curves at high temperatures over a wide range of stresses may be noted. At low stresses an incubation time appears prior to an exponential rise in the creep strain before fracture. This is more clearly depicted in the creep rate – creep strain plot of figure 3d where a minimum is reached before the creep rate increases in the tertiary stage of steel grade P92 at 650°C. The curves in the strain rate – strain plot that clearly delineates the primary stage therefore is significantly different as a function of stress. On differentiating the eq. 2 the relation

between the two axes in figure 3d can be analytically represented as $\dot{\varepsilon} = \vartheta\epsilon^{(1-\varphi)}$ where τ=1/p; φ = 1-τ; $= p^{(1+\tau)}$. This form of the strain rate – strain relation does not predict the existence of a hardening and a softening stage seen in a typical creep curve with single value of the strain exponent. Furthermore the strain exponent being dependent on the time exponent p in eq. 2, the observed stress dependence of the evolving rates is not described. The functional form to describe the individual regimes of the creep curve is achieved by providing for p < 1 for primary stage and p>1 for tertiary stage. As postulated in the power law scheme by Graham and Walles[61] a constant value of the time exponent is inadequate to describe the significantly different strain time behaviour with stress. The need therefore is use an analytical expression that explicitly provides for the stress dependence. Such an expression modified from the Wilshire – Scharning equations[69] have found wide acceptance as RCC-MR code to model the primary and secondary creep in austenitic and ferritic-martensitic heat resistant steels. The application of the RCC-MR analytical equations to model the primary stage limited to about 5% strain was shown in Eshete 1250 steel[69]. The minimum creep rate is seen to be a strong function of stress and this behavior is modelled by Norton's equation.

For the secondary stage, creep data as a function of stress and strain rate are used, as described by the Norton relation[64] shown below:

$$\dot{\varepsilon} = d\sigma^{n} \qquad (3)$$

Here, the creep strain rate is $\dot{\varepsilon}$and the stress (σ) exponent is n. This data is obtained by carrying out creep tests at various temperatures. The constant term d contains the temperature term and is proportional to exp(-Q/RT), where Q is the activation energy for creep, R is the gas constant and T is the temperature. A large number of materials have been investigated using this power law equation[71-74]. For the secondary stage where a steady state exists between the hardening and softening processes occurring during creep deformation, the stress exponent has been found to be five in case of many classes of materials (i.e. the Sherby – Dorn relationship obtained by putting strain rate terms as a steady state rate $\dot{\varepsilon}_{ss}$). This led to the term "five power law creep". However several researchers have cautioned against this generality[74]. In general however the stress exponent has been used to distinguish the underlying mechanisms of creep deformation, which has provided impetus to its popularity[74]. This is typical for the 9-12%Cr steels containing second phase particles provided attaining creep resistance. Three separate stress – creep rate regimes have been accepted to exist based on the ranges of the stress exponent values. At low stress with n ≈1 the creep deformation is attributed to take place

through migration of vacancies (diffusional creep, Harper Dorn creep). At higher levels of stress the power law region is distinguished by n values in the range of 3 – 7 where creep is believed to take place by dislocation glide overcoming the particles by climb mechanism. At even larger stresses the particles are overcome by the Orowan mechanism. This range is known as the power law breakdown region where n values are greater than 5. Figure 4 a gives a schematic plot of the regions based on the stress exponent values. The transition in creep mechanism as a function of stress is distinguished by the exponent values, which is shown in figure 4b for P92.

The applicability of the power law over a limited temperature – strain rate (steady state) range was overcome by the application of the sine hyperbolic variant of the power law[75] of the following form (proposed by Garofalo) used for high temperatures:

$$\dot{\varepsilon} = A\ exp\left(\frac{-Q}{RT}\right)[\sinh(\alpha\sigma)]^{n_g} \quad (4)$$

Various parametric models that provide a complete description of all the three stages as observed in the strain – time data obtained from creep tests have also been proposed. One of the earliest is the Garofalo equation[76] of the following form that dealt with the primary and secondary stages:

$$\dot{\varepsilon} = \varepsilon_o + \varepsilon_t(1 - e^{-rt}) + \dot{\varepsilon}t \quad (5)$$

Where $\varepsilon_o$is the instantaneous strain on loading; $\varepsilon_t$is the transient creep limit, r is the ratio of the transient creep rate to transient creep strain and$\dot{\varepsilon_{ss}}$is thesteady state creep rate.

Figure 5 shows a schematic of the plot of the actual creep curve and the one obtained from the Garofalo equation fit. It is seen that while the primary and secondary stages are adequately described, the tertiary stage is inadequately modelled by this equation.

A more complete quantitative description of the strain – time curve can be obtained from the widely used theta projection concept that fits all the three stages of the creep curve[77-79]. The form of the equation as proposed by Evans et. al[79] is tailored to describe a de-accelerating primary creep strain and an accelerating tertiary stage using the following equation:

$$\varepsilon = \varepsilon_t - \varepsilon_o = \theta_1\left[1 - e^{-\theta_2 t}\right] + \theta_3\left[e^{\theta_4 t} - 1\right] \quad (6)$$

Where ε_t is the total creep stain,ε_o is the loading strain andθ_1, θ_2, θ_3, θ_4 are fit parameters of the fit to the creep – time curve. θ_1, θ_3 are scaling parameters for the primary and tertiary stage and θ_2, θ_4 are the respective rate parameters for the former and latter stages. This concept has been used to characterize various classes of heat resistant steels and their welds. Figure 6 shows the typical fits to the experimental creep curves obtained for a type 316 stainless steel over different stress and temperature combinations. The method was originally developed for constant stress but has been also found to be applicable to constant load creep rupture test[80]. However the application of the method to Inconel alloys showed that it significantly underestimate the creep rupture lives[81]. The theta projection concept leads to an estimation of residual life using the following schemes as used in literature[82-85]: The four theta constants are determined from a set of strain – time curves obtained from creep tests carried out at various combinations of stress and temperature using the following relationship :

$$log_{10}\theta_i = a_i + b_i T + c_i \sigma + d_i \sigma T \quad (7)$$

Where i = 1,2,3,4,a_i, b_i c_i d_i are material constants and $\sigma$and T are stress and temperature of the creep experiment.

In order to relate to the creep life (time to fracture), an estimation of either the minimum creep rate needs to be done so that the Monkman-Grant relationship can be used. The nature of creep behaviour of heat resistant steels is quite different from an idealistic representation of the creep curve in the sense that the steady state stage is nearly non-existent. This is most clearly seen in the creep rate – strain plot where the curve passes through a minimum on transiting from the primary to the tertiary creep stage. Thus taking advantage of the inflection point property, the theta projection equation can be used to determine the time for attaining the minimum creep rate by equating the second derivative of creep strain expression to zero. Thus equation 6 becomes at $t = t_m$, the time to attain minimum creep rate:

$$t_m = \frac{1}{(\theta_2 + \theta_4)} ln\left(\frac{\theta_1 \theta_2^2}{\theta_3 \theta_4^2}\right) \quad (8)$$

The minimum creep rate expression in terms of the theta parameters can be written as:

$$\dot{\varepsilon} = \theta_1 \theta_2 e^{-\theta_2 t} + \theta_3 \theta_4 e^{-\theta_4 t} \quad (9)$$

While the estimation of fracture times can be carried out using the relationships in (8) and (9), the stress-temperature relationship of the fracture strain can be related as follows:

$$\varepsilon_f = a_5 + b_5 T + c_5 \sigma + d_5 \sigma T \quad (10)$$

The above relationship allows for the possibility to directly compute the fracture times at a given σ - T combination from the following:

$$\varepsilon_f - \theta_1\left(1 - e^{-\theta_2 t_f}\right) - \theta_3\left(e^{-\theta_4 t_f}\right) = 0 \quad (11)$$

Thus given a schedule of stress – temperature excursions of a component,the relations of the theta projection concept providing a model for individual material creep curves as outlined above can be used to estimate a residual life by computing a damage function. This damage function adapted from the Robinson life fraction rule is computed in the following way[84]:

$$D = \sum \frac{\Delta t}{t_f} \quad (12)$$

The residual life (R) therefore is written in terms of the creep damage D as R = (1-D)t_f where t_f is the failure life at the given stress - temperature point.

Here, the expression for the residual life from the empirical approaches relies on the evolutionary nature of a damage parameter to evaluate the residual life as a result of creep. The definition of damage depends on the estimation of a life fraction from the model equations to describe the creep curves over a prescribed temperature – stress regime. The high number of variables (e.g. 20 in case of the theta projection concept) reduces the confidence in the estimation of residual life after creep exposure over a range of temperature and stress in materials[86].

To describe the microstructure evolution during thermo-mechanical loading via a physical based approach and to compare it with phenomenological predictions, precipitation kinetics simulations as well as a dislocation density model for thermal creep using the rate theory, were applied to characterize the hardening and softening behaviour in a complex hot work tool steel[87].

The descriptions of damage developed due to creep in materials can also be developed from a phenomenological approach. A number of efforts in this direction have appeared in the literature[77,88-90]. Considering the relationship between the appearance of creep cavitation and the nature of creep curve especially for steels where the secondary creep stage is missing, it can be concluded that creep damage results in an increase of the creep rate. This rapid increase

in creep rate takes place in the tertiary stage. However, prior to the onset of cavitation damage,the degradation of the microstructure occurs for example due to particle coarsening, the appearance of deleterious phases such as Z phase or by an increase in the sub-grain size as in heat resistant tempered martensitic steels. Thus the phenomenological approach can be divided into two categories: One that explicitly incorporates the cavitation damage and the second one that deals with microstructural damage. The Kachanov model[77,90-92] is an example of the former while Dyson- Mclean[93-96] type models are examples of the latter.

The Robotnov–Kachanov (RK) equations are one of the earliest ones to use the concept of damage in the development of constitutive equations describing creep behaviour in materials. It uses a parameter 'ω' denoting damage as a scalar variable that varies between 0 to 1 as the material creeps to failure. As the creep rates at a given temperature are influenced by stress and the extent of damage developed in the material, two rate equations are required to formulate the creep constitutive equations. The first one describes the functional relation of the strain rate with defined stress and the damage parameter; the other computes the damage rate as a function of stress and the current state of damage (effective stress σ/(1-ω)). In the Robotnov – Kachanov formulation these relationships are described as below :

$$\frac{d\varepsilon}{dt} = f(\sigma, \omega) = A\frac{\sigma^n}{(1-\omega)^m} \quad (13)$$

$$\dot{\omega} = g(\sigma, \omega) = B\frac{\sigma^\nu}{(1-\omega)^\eta} \quad (14)$$

Where A, B, n, m, η and ν are temperature dependent material constants.

By integrating the equations (13) and (14), the expressions for time variation of the strain and damage parameter ω can be derived. Further applying the rupture criterion ω = 1, the failure life can be derived.

The Kachanov model has been shown to predict the tertiary creep curve of low alloy ferritic steels reasonably well[97]. However the model assumes that the primary and secondary creep strains are very small, which may be true for precipitation hardened materials at low stresses[52]. However for a broad range of materials over a large stress – temperature range this assumption is not valid. The prediction of rupture life, crucial for remaining life estimation, tends to be increasingly inaccurate at lower stresses. Nevertheless, this model is amenable to be extended from uni-axial conditions to creep rupture in a multi-axial stress state[77].

Dyson – Mclean[96] provided a framework wherein the dominant microstructural damage mechanisms that determine both creep strain and strain rate evolution during the tertiary stage of the creep curve are formulated as evolution of suitable parameters. The various forms of damage such as a coarsening of the sub-structure, a decrease in the dislocation density, particle coarsening and a stress redistribution between particle and matrix, etc. have been expressed as normalised parameters in a set of coupled differential equations (e.g. Hore et. al.[98]). The advantage of this form of creep life assessment is the fact that phenomenological relationships can be used that are well established from intensive research on the microstructure stability at high temperatures. Further there is a reduction in the number of parameters to estimate the creep behaviour (Hore et al.[98]) in comparison to procedures such as the theta projection. Unlike the damage parameter such as ω-parameter, these microstructural damage parameters are amenable for a quantification using various characterisation techniques such as electron microscopy. Thus the confidence in the extrapolation of the material parameters in the stress – temperature domain is increased by employing continuum damage models that are based on phenomenological relations describing the evolutionary nature of the microstructural damage. In this regard a microstructure based model taking cognizance of the heterogeneous polygonized dislocation network typical of the tempered martensitic steels used for heat resistant applications has been developed by Blum and co-workers[99-101] to simulate the experimental creep curve of a wide variety of materials. The model, christened as the composite model (adapted from the observations of fatigue substructures in Cu by Mughrabi[102]), treats the sub-grain network structure of these steels into plastically hard boundaries and soft sub-grain interiors. This decomposition of the microstructure into hard and soft regions, enables the application of phenomenological laws describing the strain dependent microstructure evolution in terms of sub-grain size, free dislocations spacings and sub-grain boundary thickness to determine the relative volume fraction of the 'hard' and 'soft' regions. The overall macroscopic applied stress is distributed as a local stress in the 'hard' sub-grain boundary and 'soft' sub-grain interiors in proportion to their respective volume fraction. The basis for the formulation of a kinematic framework given by Vogler and Blum[100] is the derivation of the macroscopic strain rate from the rates prevailing in the hard and soft regions on the basis of the well known Orowan relationship as given below :

$$\dot{\varepsilon}_i = \frac{b}{M}\rho_f\{v_{o,i}(T)sinh\left(\frac{b\Delta a_i\sigma_i^*}{MkT}\right)\} \quad (15)$$

$$\dot{\varepsilon} = \frac{f_s\dot{\varepsilon}_s + f_h\dot{\varepsilon}_h}{1 - \dot{f}_h(\varepsilon_h - \varepsilon_s)} \qquad (16)$$

Where i = s, h (denoting the subscripts for soft and hard regions); b = Burgers vector; M = Taylor factor; ρ_f = free dislocation density as per $\rho_f = 1/s_f^2$; s_f = free dislocation spacing; temperature dependent fitting pre-factorsof the thermally activated relationship for glide of dislocation $v_{o,i}(T) = v_{0oi} exp\left(-\frac{Q_i}{kT}\right)$; Δa_i = activation area in the hard (= bs_h; s_h is boundary dislocation spacing) and soft (=bs_f) regions; σ_i^* is the effective stress in the hard and soft regions; T = temperature; $\dot{\varepsilon}$= macroscopic strain rate; f_s, f_h = fraction of hard and soft regions; ε_s, ε_h = strain in hard and soft regions; $\dot{\varepsilon}_h$, $\dot{\varepsilon}_s$= strain rates in the hard and soft regions.

Thus from a system of ordinary differential equations describing the kinetics of deformation in the local regions that explicitly depend on the microstructure coarsening (in terms of both time and strain) the creep strain – time have been simulated not only for heat resistant steels but also for Aluminium, and Ni-based superalloy IN617[100]. Barker and Agren[103]showed that the predictive capability of the Composite model reasonably estimates creep strain of 9-12%Cr steel in the primary and secondary stages of stress rupture tests by using the Thermo-Calc software to provide estimates of thermodynamically calculated input parameters such as the volume fraction of precipitates - $M_{23}C_6$ or MX. It needs to be pointed out that the composite model does not really concern with the tertiary stage of creep in materials where most of the cavitation damage is manifested in a stress rupture tests. Nevertheless it has been successful to predict the nature of transient strains with strain rate observed in a compressive creep test.

The measures enumerated above to estimate the creep life essentially rely on predicting the strain in various stages of the creep curve by either a single empirical equation or through a set of phenomenological equations based on a mechanistic paradigm. The application of these measures to *residual life* estimation of components due to creep would entail the experimental determination of the strain – time curve from service exposed materials. This is because these measures *do no*t consider extent of material degradation of the sample selected for experiments and simply fit the response of the material obtained from a typical creep test. The only exception to this is probably the application of composite model where an estimate of creep life could in principle be carried out just by the knowledge of the nominal composition, heat treatment and service conditions that need to be well known beforehand[78]. For residual life calculation, however, the nature of microstructure evolution should be well known and described in the constitutive behaviour framework. In the absence of such a knowledgebase the

reliable alternative is to undertake comprehensive service monitoring using say service exposed samples. Thus a set of rupture tests (using suitable stress – temperature combination) carried out on sample extracted on component material at different points in the service life can be used to create a database of the creep curves as a function of its exposure to service conditions. Using a systematic application of the various types of model equation a functional relationship would then be developed between the fit parameters and the exposure time which could then be used to estimate the residual life. In this form the fit parameters essentially serves as an index of the service exposed condition, which will be specific to the microstructure of the sample extracted from the component. It is thus assumed that the microstructure that has evolved within the sample volume randomly selected from the component is representative of the volume of the component so that the residual life computed can be used to develop protocols to aging management. It is to be pointed out here that such a testing program invariably would be short term carrying out rupture tests at suitable combinations of stress – temperature expected to last about an order of magnitude of shorter duration as compared with the expected creep life. Thus there is need to use alternative schemes for extrapolation, typically of the form given below

It is well known that creep in materials results in microstructural degradation and development of damage in the form of cavitation. These phenomena are quite localised and sensitive to the fluctuations in stress and temperature. Thus the use of data from full sized sample picked from arbitrary suitable location of service exposed components for the purposes residual life assessment may not contain representative volume affected by creep degradation. One way to increase the confidence that a full volume sample also contains representative creep damage is to extract it from regions of the component having high probability of failure. Thus the monitoring of accumulation of strain in high temperature components using online and offline methods could be used to determine target regions for extraction of samples[77]. The methods include providing for some fiducial markers on the component surface that would unaffected by oxidation such as peening or by attachment of capacitance gauges. Other possible methods include ultrasonic techniques to assess section thickness reductions or imaging the surface of the component by stereo-photography or laser holography. The measurement of strains on the component are however quite challenging as the deformations must be measured in confined spaces with reproducibility and resolution of nearly a thousandth of a percent with typical strain rate measurement capability of the order of 10^{-8} – 10^{-9} h^{-1} [73]. These requirements notwithstanding, the implications of extracting a volume of ~ 1000 mm^3 suitable for making

tensile sample of 5-8 mm gauge diameter on the function of the components, may be unacceptably severe as it would superimpose on the present damage process due to high temperature exposure.

The residual life assessment of components in the plant using service exposed samples needs therefore to be evaluated using much lower sample volumes. In this regard two broad based approaches have been developed. The first one uses the phenomenological relations describing the microstructural evolution kinetics[59] and second approach uses the miniature testing technology[79], both of which imposes drastically reduced sample material volume requirements for residual life assessment. For example the typical features of the tempered martensitic / bainitc microstructure of heat resistant steels that were amenable for quantitative characterisation have been the compositional changes of second phases such as cementite[105,106], appearance of various classes of fine precipitates such as transition carbides and tracking evolution of lath[107] and sub-grain sizee[108]. In these steels the cementite second phase composition is far from equilibrium[59]. Therefore prolonged exposure to elevated temperature would drive the cementite composition with respect to substitutional elements towards equilibrium levels. Thus by assuming the growth of cementite under para-equlibrium conditions the enrichment of the phase by elements such as Cr has been shown to follow parabolic kinetics experimentally monitored over about ~ 100 hours during high temperature exposure during say the tempering step[109]. Another possibility to track the extent of microstructure degradation is by monitoring the volume fraction of different classes of transition carbides found in modern alloy steels eg. NF616[59]. The advantage of using the alloy transition carbides is that their evolution continues to occur well into the tertiary stages of creep. Thus, while extrapolating the coarsening kinetics of second phases such as cementite characterised over few hundred hours by almost 3 orders to magnitude to ~ 1-2x10^5 hours may be unrealistic due soft impingement effects that limits particle growth by diffusion, the micro-analysis and quantification of the fine transition carbides that continually evolve right upto the end of life may have more realistic value for residual life estimation. However as shown by Hofer et. al.[110] due to the fine nature of these particles considerable uncertainty is introduced in the identification and quantification of these particles (eg. MX and $M_{23}C_6$ in G-X12CrMoWVNbN10-1-1 after 33000 hours creep at 600°C) using conventional TEM. Apart from the particle coarsening the fine dislocation structure in tempered martensitic steels also has been found to coarsen and an unique growth law of the sub-grain as a function of strain of the following form has been proposed by Blum and Gotz [108] at constant stress and temperature.

$$\varepsilon = 0.12 \ln\left(\frac{\log\left(\frac{w_0}{w_\infty}\right)}{\log\left(\frac{w}{w_\infty}\right)}\right) \quad (17)$$

Where w_o, w_∞ and w are initial, steadystate and measured sub-grain sizes respectively.

The coarsening of the sub-grains can thus be directly related to the strain and residual life estimated once the strain – time curve is known.

The microstructural approach is limited by the extent to which the phase/ precipitate coarsening relationships can be extrapolated to end of life with confidence. Thus recourse to miniature testing techniques, is quite inevitable from the view point of economy of sample volume that does not compromise the integrity of the component. In the miniature testing two approaches can be adopted[104], one that miniaturises the sample design used for full scale testing and the other that uses innovative sample designs such as punch testing methods. The miniature testing methodology originally developed for post irradiation mechanical properties of nuclear reactor vessel materials was first applied by Parker et. al[111]. to estimate the creep properties of low alloy steels. The miniature sample creep property techniques now include small punch, impression and small ring creep tests[104]. Amongst these the extensive use of the small punch tests is mainly due to the fact that life information can be determined as the test takes the specimen to failure. The typical nature of curve from small punch creep test remarkably shows similarities with the creep curve from full size specimen. This is surprising considering that the punch deformation mechanisms are significantly different from the conventional stress rupture test[112,113]. The curves obtained from SPCT in the punch displacement – time format at a constant load for a given test temperature can be divided into three distinct stages of deformation[70]: initial acceleration of punch displacement under the action of high local stresses caused by low contact area between spherical punch – specimen and the low bending rigidity of the latter; followed by the stage where the punch displacement remains stationary minimum rate as the local stresses decrease due to greater contact of the punch – specimen and increase in the bending stiffness of specimen; finally near the end of the test a rapid increase in displacement rate due to progressive development of geometrical instability caused by the propagation of cracks and damage. The failures in SPCT have generally been found to occur away from the load line and in the circumferential direction suggesting membrane stretching failures[114]. As is evident from the above, the mechanisms related directly to dislocation motion and formation of damage that determine the deformation rate in uniaxial creep are not the same as in SPCT. Despite this as pointed out earlier the similarity of the experimental curves gives

confidence that residual life approaches that parameterize the creep strain verses time curve can be applied to estimate residual life. As an example the following equation set provides a direct empirical relation between the minimum displacement rate and minimum strain rate and combining it with the Monkman Grant relation to estimate the residual life[115].

$$\dot{\varepsilon}_s = 10^{(C - C_s/m)}\dot{\Delta} \quad (18)$$

$$\log t_f + \left(m_s log\dot{\Delta}\right) = C_s \quad (19)$$

Where $\dot{\varepsilon}_s$ = minimum creep rate in the rupture test; $\dot{\Delta}$ = minimum displacement rate in the SPCT; C,m = Monkman Grant constant and exponent respectively obtained from rupture test; C_s, m_s = Monkman Grant constant and exponent respectively obtained from SPCT.

A rigorous post analysis step of the SPCT is required to determine the stresses and strains in order for the results of the test to be related to the conventional creep tests. This has been achieved notably by the various analytical methods such as derived from Chakrabarty[116] membrane stretching model and computational approaches using FEM to virtually simulate the test[70]. As is obviously evident significant empiricisms are endemic to the use of these miniature test specimens as they are attempt to relate macroscopic test variables such as displacement rate, strain, strain rate, stress etc across a large length scale of deformation occurring under very different imposed stress states. It would be therefore naturally better to have a physically measured parameter that bears a direct relation to creep failure. While it is believed that creep cavitation occurs only at the late tertiary creep stages a number of studies with regard to 9-12%Cr heat resistant steels attribute the onset of damage, visible by optical microscopy or SEM, near to strains at the minimum creep rate. Thus in these classes of steels while most of the time will be spent in attaining the minimum creep rate, the accumulated strain or creep ductility will be largely dependent on the progress of damage by cavitation. As a result, if the knowledge of strain to failure at different stress – temperature combinations occurring in large samples could be related to the measurable parameters of damage developed in the material, a vastly improved index of transferability criterion of failure from component to full scale and miniature sample could be developed. This approach of assessing the residual life due to creep by defining end of life using a suitable criterion of quantifiable damage could be assessed using both full scale and miniature specimen tests seamlessly. As pointed out earlier this could not be contemplated until recent rapid development in the micro-tomographic technique. The following section

presents a brief summary of the nature of information that could be obtainable from the application of tomographic characterisation carried out principally on small samples.

4. **Fundamental nature of creep cavitation in 9-12% Cr heat resistant steels**.

It is clear from the preceding sections, that 3D characterisation of damage provides unambiguous information and that the existing methods are quite inadequate to estimate the residual life as they heavily rely on phenomenological or correlative relationships. Furthermore the rapid development of the tools to carry out complete 3D characterisation of engineering materials exposed to degradation phenomena such as creep now have the capability to interrogate the bulk on multi-modal and multi-scale basis. This is most pertinent in case of creep as the microstructure coarsens in terms of increase in sub-grain and particle size and thus influences development of cavitation from its incipient stages in the nano-meter level to millimetre length scale. However, some technique of integrating the destructive and non-destructive 3D methods needs to be evolved. The latest development of the concept of Correlative Tomography proposed and developed by Burnett, Withers and co-workers[117] is a step in the direction of combining multi-scale characteristics of damage. Based on the existing concepts of Correlative Microscopy, the Correlative Tomography seeks to delineate a common volume of interest where the damage imaged from micro-CT in the micro-meter length scale and micro-voids in the sub-micro-meter length scale obtained using FIB-SEM have been correlated with crystallographic orientation relationships from SEM-EBSD and chemical mapping from TEM elemental analysis. Such exemplary convergence of multi-modal information over length scales are expected to reveal new insights into the mechanisms of failure phenomena such as corrosion and creep damage. The relevance of such a technique for residual life estimation would be to provide means to reduce the correlative burden to establish the equivalence of the damage processes in samples with different extents of miniaturisation. In order to do this it is important to know the characteristics of creep cavitation in 3D for heat resistant steels which is the concern of the present section.

The steel chosen for the investigations was a tempered martensitic steel CB8 (10.8% Cr) developed in the COST program[28]. The creep tests were carried out at 600°C over the stress range 120 – 180 MPa. Small sample coupons extracted from near the fracture surface were subjected to micro-tomographic scanning at BL20XU beamline of SPring-8. The 3D visualization of the datasets (Figure 7), their quantitative analysis and combining the tomography dataset with that obtained from serial sectioning revealed new insights into the

fundamental nature of creep cavitationin heat resistant steels. The wide stress range over which the samples were crept and subsequently subjected to micro-tomography experiments provided a unique set of 3D data that captured the transition of failure from trans-granular to inter-granular mode. This was manifested by a sharp decline in the fraction of life where cavitation processes dominate as seen in the Figure 8 from the quantitative analysis of the datasets. Figure 9 depicts it is obvious that as a function of creep exposure time all the metrics of cavitation increased. Thus it can be concluded that with an increase in creep exposure time the intensity of creep cavitation increases in tempered martensitic steels. Considering the fact that the rupture ductility as a function of stress and creep exposure time (figure 10) significantly decreases and also the fact that the observed creep cavitation has intensified within a lower fraction of creep life, this could signify an hitherto unknown manifestation of creep damage in heat resistant steels as the mode of failure changes from trans-granular type to inter-granular type.

The 3D dataset obtained by high resolution micro-tomography scan on sample coupons extracted from crept specimens of CB8 scaled in high temperature exposure ranging from about 120 days to about 6 years could contain trends revealing the fundamental nature of creep embrittlement in heat resistant steels. In contrast the in-situ tests carried out on brass[112] and copper[102,103,106] provide information on short term creep properties which in case of steels are inadequate to capture the creep embrittlement phenomenon in heat resistant steels that occurs at long term exposure at elevated temperatures. Further, it is long known that internal interfaces such as prior austenite boundaries, packet and lath boundaries are preferable sites for the creep voids. Imaging these features in absorption tomography is not possible. Other techniques such as holo-tomography, diffraction contrast tomography or 3DXRD can be used for this purpose[28]. Serial sectioning method on the other hand is a simple and relatively inexpensive repetitive technique to capture the microstructure in 3D. Combining the two techniques of absorption tomography and serial sectioning to create a multimodal 3D dataset would reveal the importance of the internal interfaces. Therefore for the creep damage characterization of CB8, the two techniques have been combined to provide an idea of the importance of prior austenite boundaries.

The 3D visualization of the datasets obtained from the tomography scanning of the sample coupons reveals a very in-homogenous distribution of the creep voids at rupture within the stress range 120 – 180 MPa. Figure 8 shows three datasets obtained from samples crept at 120 MPa, 150 MPa and 180 MPa. The increase in clustering of the voids is clearly seen in the crept

volume characterized by micro-tomography at 120 MPa, which had the longest high temperature exposure. The close up rendering of the ensemble of creep void cluster shows their complex arrangement around a large multiple lobed oblate shaped voids (figure 11). Other regions in the dataset show many creep voids arranged as a chain, which are either one or two lobed. Regions in the dataset have also shown clusters of multi lobed voids. These complex morphological shapes suggest that an evolutionary behaviour could be ascribed where the coalescence process seems to increasingly dominate. A survey of the shapes within the dataset tentatively suggests that the morphology of voids evolve from growing singly to first a double lobed shape and then transitions to multi lobed cluster and ultimately forms a large coalesced void. The regions containing these high densities of complex shaped voids could be conjectured to be approaching "instability" in the cavitation behaviour that ultimately transforms to cracks leading to creep fracture. The trend of these results suggests that the coalescence affected fraction of the voids within the dataset increased as the creep exposure times increased. Due to the absence of direct evidences of coalescence as seen in an in-situ experiment by continuous tomography, an indirect method based on the changes in the sphericity parameter was used to estimate the coalescence affected fraction.

The coalescence-affected fraction was estimated from the unique behavior of sphericity that alternates between acicular to spheroidal morphology as a function of size. Such a behavior was rationalized as one that could possibly occur if growth and coalescence of voids present in the various internal interfaces take place under the influence of grain boundary sliding. Thus this trend implied a negative correlation of the sphericity with void size which was then used as the criterion for assessing the coalescence affected fraction by identifying the critical void size beyond which the coalescence occurred. Figure 12 shows the analysis and construction of the plot used to estimate void coalescence fraction for the dataset obtained from sample coupons extracted from a specimen crept at 120 MPa. The variation of the coalescence fraction with exposure time is plotted in figure 13, where the increase is clearly revealed. This increase in the coalescence of voids could be responsible for the observed increase in clustering. This could be inferred from the fact that the clusters contained void sizes that were greater than the dataset average.

The application of serial sectioning on the dataset obtained from a sample coupon crept at 150 MPa showed that the distribution of voids were predominantly near the prior austenite boundary. At 120 MPa, however, the rapid proliferation of creep voids within the volume was clearly evident. A scatter diagram of the voids observed is plotted in figure 14 to show the

spatial distribution of the voids and their relation to the large coalesced voids of increasing volume. It can be clearly seen that the voids proliferate along lines, which have been drawn by visual inspection. Considering the fact that the prior austenite grain size of the samples crept at 120 MPa was 600μm, which was far less than the coupon dimensions, the rapid increase in cavitation could be ascribed to grain interior cavitation. This gives a new insight that cavitation at packet and lath boundaries leads to a sort of "instability of creep voiding" at prior austenite grain boundaries, which hasten the onset of creep fracture. As a result the lowering of creep life, ductility and change of failure mode from trans-granular to inter-granular occurs. This transition in cavitation mechanism in long term creep of heat resistant is illustrated schematically in figure 15 and can be ascribed to be the fundamental nature of creep cavitation in tempered martensitic steels.

The steel grade E911, a martensitic 9 – 11%CrMo(W)VNb used for steam power plant components such as boiler tubes, headers and turbines was crept under multi axial conditions using a plain pressurised hollow tube to simulate the service conditions of in-homogenous multi-axial loading[118]. A tomographic investigation was carried on a sample (diameter 600μm and 2mm long) extracted in the radial direction from a specimen of E911 crept at 600°C for 37800 hours under multi-axial loading conditions imposed by an axial stress of ~ 49 MPa, and internal pressure of 17.7MPa. The damage seen in the form of a distribution of cavities across the cross-section and length of the sample was quantified in terms of void density which was found to nearly uniformly distributed (Figure 16(a)). The void morphology was described by a set of metrics that could discriminate between coalesced and non-coalesced voids. The size distribution of the non-coalesced voids successfully fitted a theoretically derived equation due to Reidel[119] with the exponent $\beta \sim 2$ (Figure 16(c)). This suggested that the void growth mechanisms to be constrained diffusional mechanism. Similar results were obtained for the tomographic investigations on samples extracted from a *notched* hollow tubular specimen crept at 575°C for about 80% of lifetime under axial stress of ~62 MPa and internal pressure of 17.5 MPa[120]. However the presence of notch not only rendered the distribution of the voids to be in-homogenous but also showed a four-fold (from ~ 17000 in plain hollow cylinder to ~ 70000 in notch hollow cylinder) increase in the population of un-coalesced voids. The mapping of the variation of the number of the creep voids along the length showed that it peaked at a distance of about 0.8 from the inner surface. It is however to be pointed out that the higher number voids quantitatively analysed for the case of notched hollow specimen from its plain counterpart may be due to the difference in threshold voxels defined in the respective datasets. The in-

homogenous void distribution as a result of the notch was investigated with the variation of local stress parameters such as von mises stress (VMS), Maximum principal stress (MPS), and principal facet stress (PFS) as well as the stress tri-axiality factor. The estimation of these scalar stress parameters were carried out using FE simulations incorporating the viscoplastic Norton's law to describe the creep of the notched hollow specimen. The relative importance of these stress parameters on the void nucleation and growth were evaluated using a cross-correlation coefficient with the variation of void volumetric density. It was concluded that stress triaxiality factor (due to notch) along with VMS & MPS significantly influence the development of creep damage in E911. Compositionally additions of W to E911 has been found to be beneficial for creep resistance as compared with P91 (that does not contain W). With the aim to compare the development of creep damage in these two steels and possibly to reveal the influence of W on creep cavitation, both materials have been subjected to tomographic studies[118]. The sample of P91 steel was extracted from a plain hollow specimen crept at 575°C for 10200 hours under an axial load of 53 MPa – 24 MPa internal pressureand compared with the tomographic results obtained for the corresponding E911 steel sample mentioned above[118]. The quantitative analysis of the dataset showed a significant increase in the void content increasing from about 17000 non-coalesced voids for E911 (volume ~ 0.7 mm^3) to about 42000 for P91 (volume ~ 0.9 mm^3). Consequently the void density along the length of scanned sample volume was higher for P91 as compared with E911 (Figure 16(b)). Considering the creep conditions in terms of temperature and exposure for P91 to be less severe than E911, owing to the slightly higher values of scalar stress parameters of VMS and MPS for the latter, the significant increase in the number density strongly implies that the propensity for nucleation of voids are easier in the former steel. As the creep exposures were not same for the two steels, using a void growth equation consistent with the constrained diffusion mechanism, it was found that the final growth sizes to be similar at creep time of ~ 10000 h for both the steels. This suggests that the presence of stabilised $M_{23}C_6$ and laves phase by W in E911 does not influence the creep void growth rate. These microstructural differences however can influence the void nucleation as it was estimated that P91 contained at least thrice the number of voids per unit grain boundary area. This could be attributed to the pinning of the grain boundaries by the inter-metallic laves phase to prevent sliding, a well known mechanism of void nucleation at these low stresses.

The creep behaviour of welded 9-12%Cr heat resistant steels has also been investigated at large synchrotron source, in new experimental steel with modified compositions as compared with

P92, principally by additions of controlled amounts of B and N[121]. The steel called as MARBN was compositionally designed for imparting enhanced resistance to Type IV cracking in cross welded components by suppressing the formation of a region of fine grain in the heat affected zone. The achievement superior creep resistance as compared with P92 at low stresses below 100 MPa was not realised and hence the investigation on the nature of damage and its spatial distribution was attempted to be investigated by micro-tomography. For this purpose small coupons (450μm x 450μm x 10 mm) from welded samples crept at 650°C over the stress range 70 – 150 MPa were extracted to contain the weld, HAZ and base metal. From the tomographic scans it was clear that as the stress was lowered, there was increase of cavitation in a narrow zone away from the weld (figure 17). The spatial closeness of the voids and their morphology suggested that their presence was due to coalescence of closely spaced voids. This also implied cavity nucleation in this zone was easier. Complementary EBSD studies (figure 17) showed that the zone contained fine grains near individual PAGB. These studies provided the insight that while the compositional modification are able to eliminate the region of uniform fine grains, these individual PAGB could contain fine grains which became sites of localised concentration of cavitation at low stresses leading premature failure of cross-welds.

These studies reveal that the fundamental nature of cavitation is manifested most intensly in heat resistant steels at stresses of 100 MPa and below. This stress regime is important as compositional design has been successful in bringing expected increase in creep life at higher stresses where the volume and number density of creep voids are significantly lower. High resolution micro-tomography at large synchrotron sources reveals the voids assume a very complex morphology from early tertiary stages and tend to localise at grain boundaries. The spatial distribution is thus rendered highly in-homogenous. Heat resistant steels being martensitic, the presence of large number of internal interfaces provide additional void nucleation sites that cannot be influenced by secondary phases such as Laves phase. At failure the tomography scans show that even within regions far from crack a significant fraction of the voids are affected by coalescence, which are most strongly manifested in the welded materials deduced from multi-lobe morphology of the voids. Furthermore the spatial heterogeneity of cavitation cause local stresses to be significantly altered which needs to be assessed from application of FEM as they have significant influence on the evolution of creep damage. The prediction of the creep life in this low stress regime would thus require the development of knowledgebase describing the relations between cavitation content and morphology, microstructure and local stress.

5. **New directions of residual life estimation in the light of the fundamental nature of creep cavitation in heat resistant steels**

In the previous sections detailed critical survey of the methods of creep life estimation showed the inadequacy to describe the basic nature of the plot between strain – time obtained from a laboratory test. Three classes of residual life estimation methods ranging from empirical equations, parametric model equation and continuum damage equations, which have been extensively applied to heat resistant steels were reviewed. In all the methods the functional relationships between the nature of damage and creep life were found to be wanting. Whereas the empirical and parametric equations relied on the evolution of macroscopic quantities such as strain and strain rate (e.g. creep damage parameter), that were indirect measures of creep damage, explicit incorporations of creep damage into constitutive equations to estimate residual life lacked a satisfactory definition. In the RK formalism the creep damage parameter denotes an effective cross-section loss variable due to the presence of creep voids. This parameter has a maximum value of 1 denoting that loss of cross-section is complete at rupture. This approach illustrates the classical assumption of the CDM approach wherein a single variable is thought to represent the state of damage that is developed in the material due to degradation phenomena such as creep. The multitude of mechanisms during creep degradation has been incorporated in physically based CDM equations by Dyson and co-workers[27, 93-96]. These equations are however phenomenological and the nature of the functional relationship is not based on the any quantification of creep damage. The cavitation led failure is most strongly expressed at low stresses which have been clearly revealed by the application of tomographic characterisation of long term creep exposed samples of 9-12% Cr heat resistant steels. The creep embrittlement is most severe in the stress range below 100 MPa where continuum damage approaches such as RK method are quite unsatisfactory to predict the creep life.

In view of these shortcomings of the analytical equations such as Garofalo, Theta projection etc. describing creep curves obtained from laboratory experiments, the alternative option is to carry out examination of the service exposed material for assessment of residual life. In this way to estimate residual life a suitable material characteristic is monitored, which when reaches a critical value the results in exhaustion of component life. A number of material characteristics which includes mechanical parameters (such as hardness, tensile test, miniature test, strain monitoring) and microstructural parameters (inter-particle spacing, cavitation, cavity number density and volume, miss-orientation measurements) have been proposed that serves as an index of life expended due service exposure. The most reliable has been the miniature testing

techniques such as small punch creep test as they mimic the creep curve obtained from a full scale test in the laboratory. The creep test being a time consuming one and the task of residual life assessment being a comparatively expeditious one, the choice of parameters, amongst the multitude indices listed above, optimises the economy of effort and reliability of the estimation. For example microstructural parameters obviate the need for re-testing and extraction of a significant volume of material from component. However considering the heterogeneity of the coarsening of particles and sub-grain network and the tenuous extrapolation possibilities limited by the physical constraints of diffusion controlled growth of precipitates, the reliability of the end of life criteria based on microstructural parameters is poor. Thus an effective compromise is the small punch creep test that provides an accelerated test to failure yielding a remarkably similar nature of plot as a standard creep test. However, as it is well known that the nature of deformations in small punch creep test is significantly different from those in uni-axial creep their applicability rests on the strength of a correlative study. The applicability and usefulness of the tomographic characterisation of creep damage in these issues of residual life estimation are significant. The application of micro-tomography provides a tool for direct characterisation of creep damage in a quantitative manner. Hence it is able to provide characteristics of cavitation such as volume number density and size estimation that can be used to define the cavitation parameter for use in the constitutive creep damage constitutive behavior. Further the relation of these cavitation characteristics provide functional relationships with exposure time, stress and rupture ductility that can be then used without any ambiguity for estimating creep life over a range of stresses. In the case of CB8, the investigations of Gupta et. al.[28] provided a quantitative relation between void volume fraction and number density with rupture ductility over the stress range 120 – 180 MPa. The relation of rupture ductility with time of failure is quite direct and hence using the quantifiable results of tomographic characterisation of creep cavitation, a vastly reliable parameter of life estimation is formulated. Further, as already pointed out the tomographic technique is amenable for 4D characterisation through in-situ tests. Thus these relatively short term in-situ tests could be a viable alternative to the SPCT that could provide new monitoring criteria based on evolution of quantifiable cavitation rates. Thus the definitions of end of life would be based on quantifiable characteristics of cavitation determined by application of micro-tomography. This would considerably enhance the reliability and accuracy of the residual life estimation method.

It is well known that extrapolation creep life over a wide range of stress provides a great challenge owing to the complex behavior of cavitation as the mode of failure transitions from

trans-granular mode to inter-granular mode. One way to treat this transition is to evolve criteria for the onset of cavitation instability characterized by a sharply reduced time scale from nucleation to coalescence of the creep voids. The onset of cavitation instability provides the nucleation of cracks that then leads to treating the residual life from the view point of fracture mechanics approaches such as C_1^* (the steady state creep analogue of J[122]). Thus with the application of synchrotron micro-tomography an effort to design a framework for a unified approach combines the damage mechanics approach and fracture mechanics approach. This can be made to estimate the residual life on the basis of quantitative 3D parameters, which are physically relevant with much reduced empiricisms.

It is thus clear that the application of the tomographic technique would yield exemplary information that is directly connected with cavitation process responsible for creep failure in materials. In heat resistant steel there is strong evidence that low stresses (near to 100MPa and below) cavitation begins very early in the tertiary stage at strains close to the minimum creep rate at a given stress and temperature. Thus the accumulation of creep strain can be considered to primarily due to progress in cavitation in the heat resistant steels. The measurement of strain is quite basic to the residual life assessment of component. This is because strain accumulated indicates the extent of creep undergone by the steel at a given stress and temperature, and its measurement could provide a basis to connect lab and component manifestations of degradation. Even for the correlative relation of Monkman- Grant relation between minimum creep rate and time to failure in creep curves for a number heat resistant materials including steels, is more appropriately described by explicitly incorporating strain to failure[123]. However it has been found that the measurement of strain at the component level and at lab using full scale sample or miniature samples does not bear a direct interrelationship. Thus transfer the lab based estimates of life to the component is one of un-certainties associated with residual life methods. The second key issue is whether the lab based samples full scale or their miniature variants are able to contain a representative volume in which the degradation process is manifested under the applied stress and temperature. This issue is of concern especially for creep where sample size can influence the manifestation of creep mechanism. For example it has been shown in aluminium alloy that the mechanism of creep changes from Harper – Dorn to Power law depending on the specimen thickness to grain size ratio[104]. Therefore the critical assessment of the applicability of the tomographic technique for residual life estimation needs to revisit this key issue of statistical robustness the data from small volumes.

The requirements of the miniature specimens for various mechanical property determinations have been discussed by Hyde et. al[104]. in an exhaustive review where the issues, limitations and approaches adopted to take advantage of the benefits of small specimen test are summarised to determine yield strength, creep, fatigue, and toughness properties in materials. In general the guideline the use of the definition of a full scale specimen in terms of the microstructural unit of grain size is to contain about at least 8-10 grains across the section and about 200 - 8000 grains in its volume. The determination of mechanical properties such as tensile properties and modulus from such sample has been taken as representative of the bulk. The implications of these criteria for applying the miniature samples for evaluation of these mechanical properties would be to provide a lower limit to their size. Yet another criteria that is related to the volume is the evaluation of strength materials containing a defined distribution of damage, a typical example of which are ceramics[104]. This relationship between volume of materials containing damage and strength has been quantitatively given by Weibull in terms of a probability of failure[104]. This relationship essentially describes the damage content sampled in terms of the volume of material tested. Therefore the strength parameters obtained from miniature samples can be corrected by simply scaling up the volume. Miniature samples also have another difference from the established large samples to evaluate properties such as fracture toughness which are obtained from multi-axial conditions. The constraint imposed on the volume of the miniature samples are quite relaxed especially for low yield strength materials due to large plastic zone size. The development of constraint is also depends on the heterogeneity of the microstructure as typically seen in welded heat affected zones where a weaker region develops between the weld and base metal. Between these two forms of constraint – one that arises from the imposed stress state and the other that is intrinsic and independent of the external stress state, a common effect of altered local mechanical properties is created that provides significantly values of mechanical properties different from the bulk properties. While the former can be corrected for using computational approaches such as FEM or statistical approaches such as Weibull (as in low temperature fracture toughness using Master Curve approach), no procedure can directly correct for the latter except for choosing sufficient volume of sample (such as weld metal to sample diameter ratio > 1). Although for the measurement of creep properties Hyde et.al[104] have limited the concerns to ensuring adequate number of “elements” (to be interpreted as grains) in the miniature samples, for assessment of residual life all of the issues are relevant. This is because an extracted sample from service exposed component would contain both damage and microstructural heterogeneity.

Considering the fact that two broad types of miniature specimen have been in use, one that reduce the dimensions of the standard design of full scale specimen and the other use innovative specimen design (such as disk specimen for SPCT), the representative volume criterion for containing adequate number of elements are fulfilled as the modern structural materials contain grain sizes of the order of 30 -50 μm. It is therefore not surprising that the creep tests carried out in the inert gas (to avoid oxidation) on sample diameters from 5 mm to 2 mm on CrMoV steel show similar creep curves[104]. Even for the SPCT samples containing different extents of prior damage extracted from specimens subjected to increasing creep exposure, there is systematic decline in duration of test and increase in the punch displacement rates[104]. Thus their suitability to estimate remaining life is quite encouraging. The typical dimension of disk sample for SPCT test are about 6 – 10 mm diameter with 0.5 mm thickness and uses a punch diameter of 2mm. These typical dimensions of the sample also are able to satisfy the representative element number criterion provided significant coarsening of the grain size has not occurred. While this would not be an issue for short term creep exposure, in case of long term crept samples where significant increase in grain size has occurred (eg. Increase in grain size to 600 μm for CB8 after 54000 hrs) the issues of applicability of the small sample would have to be considered. Thus there could be an upper limit of the extent of creep exposure that is relevant to the use of SPCT to yield useful information for remaining life studies. This limitation superimposes on the general challenge that SPCT tests provides on estimating the parameters of constitutive equations for estimating remaining life (i.e. stress and strain) from the load and punch displacements. The correlative framework that the SPCT method needs to relate the creep behaviour of the material has been heavily dependent on the analytical or computational approaches (FEM) to determine the strain and stress evolution during the test from the load – displacement data.

The application of tomographic technique for residual life assessment is based on the using the knowledge of creep cavitation characteristics revealed by 3D imaging of material volume to construct suitable end of life criteria. In case of steel samples, a cross-section typically in the range 300 x 300 μm^2 to 600 x 600 μm^2 have been imaged at high resolution of 1 μm at large synchrotron sources. At these resolution levels a very large number of cavities (upto about ~ 50000) have been reported to be detected in 9-12 % Cr heat resistant steels at 3rd generation synchrotron sources (ESRF) in typical volumes of the order of 1 mm^3 characterised by montage tomographic scans of contiguous regions[118,120,121]. Therefore the characteristics of creep cavitation such as volume fraction, void density, void – void distance, morphological metrics

etc. have sound statistical basis and can be used for a design suitable criteria to retire components. However, as creep damage is heterogeneous in nature the spatial assessment of such characteristics is required at larger volumes. On relaxing the resolution requirements a considerable larger volume of the sample containing damage can be imaged, as for example visualising in 3D, the etch pits in a stainless steel rod of 2.5 mm diameter and ~ 5 mm length contained within the volume due to localised corrosion[117]. The implications for detection of creep cavitation via tomography at marginally reduced resolutions are quite significant as the volumes being characterised would qualify to be representative of the bulk for determination of mechanical properties. The concern that reduced resolution (say from 1μm to 3μm) could lead to a loss of information seems to be largely unjustified, at least, looking at the results from CB8 investigations. This is because the analysis of 3D creep cavitation data yielded that the coalescence affected fraction of cavities, that contributed to the majority of the bulk volume fraction of voids began only after 4μm. At reduced resolution, while it has been possible at large synchrotron sources to provide penetration on significantly larger cross-sections on light metal alloys (1.4 x 1.4 μm^2 on MMC: Buffiere et. al.[94]) such an exercise for steels correlating the resolution to the sample volume has still to be reported. As pointed out the emergence of the destructive 3D techniques provide further alternatives to determine the 3D characteristics of damage at larger volumes. These techniques based on serial sectioning techniques were earlier applied on small volumes (eg. 3-5 x 10^{-3} mm^{-3} by Kral and co-workers[50,51]). At these volumes the coarsend grain structure (~450μm size) could analyse only a few grains. However the capabilities of serial sectioning technique to capture extended volumes at 0.5μm resolution have been also reported[124]. The application of serial sectioning to extended volumes requires intensive manual intervention to create a high fidelity 3D dataset. Recently with the development of new complementary 3D techniques, such as large field serial sectioning and concept of automated work flow, these techniques can now considerably aid to augment the information on cavitation damage derived from its non-destructive counterpart of micro-tomography. The latest technique of correlative tomography provides a glimpse of such protocols that aim to complement the destructive and non-destructive techniques[117]. Thus for the application of residual life assessment using micro-tomography various approaches can be adopted for increasing the characterised regions of the material so that it fulfils the representative volume criterion. These include contiguous tomography scanning of adjacent regions, serial sectioning of large regions of sample such as montage or large field serial sectioning, and integrating destructive and non-destructive 3D techniques so that multi-modal

end of life criterion can be developed. In this regard for assessing purely residual life due to only creep, extraction of sample near to cracks may be inappropriate as the damage developed would significantly be affected by plastic localisation. However the analysis and integration of such information are useful for a realistic life determination of component where creep cavitation engenders crack formation and growth under the influence of enhanced damage gradients. In this the role image based modelling of an identified architecture of damage would be useful for estimation of life of component. Such an exercise can also assure the transferability of the cavitation characteristics determined from the sample to the component,. As these image modelling directly work on the 3D cavities reconstructed from the tomographic scan on sample extracted from the component, the results of the computations can be directly used with the interpretations of FEM or Stochastic simulations[125]. This contrasts with assessing the residual life where the experiments on miniature sample yields a punch displacement verses time curve which needs to be processed using analytical models or FEM to transform the plots into stress and strain relations so that creep life estimating parameters of the constitutive equations could be computed. In this approach there is no direct scale up to the component level, as is possible by application of the tomographic approach. Finally, the issue of heterogeneity of microstructure that is relevant to the applicability of miniature sample for residual life estimation needs to be addressed. The tomographic method provides not only quantitative information on the cavitation characteristics but also provides the spatial distribution of the cavities within the volume. If the volume of interest is representative of the bulk, an unit architecture of cavitation could be delineated for image analysis. In this manner the heterogeneity of the microstructure and attendant damage can be directly factored in the residual life calculations. Again it can be pointed out that such an exercise has yet to be undertaken. In conclusion, it can be said that while the tomographic method to estimate residual life has definite advantages by being the most suitable to define an end of creep life criterion in terms of cavitation characteristics, its applicability to be assessed from small volumes has still to be demonstrated. In this endeavour the recent development in destructive 3D techniques, image modelling and correlative tomography protocols have to be combined to realise this potential of the tomographic technique for assessment of residual life of components.

6. Conclusions/Summary

The phenomenon of cavitation in long term crept heat resistant steels are quite complex which is being revealed by a growing number of studies using micro-tomography. As a function of stress, the well known transition in the transgranular to intergranular mode of creep failure in

heat resistant steels is now revealed to be due to an explosion in the cavitation characteristics in terms of volume and density, as interpreted from the tomographic investigation of CB8. The spatial analysis of the evolution of the cavitation behaviour indicated that grain interior cavitation influenced the progress of creep damage at the grain boundaries. Similar mechanistic insights on the growth and coalescence behaviour of creep cavities have been revealed under multi-axial conditions in other grades of heat resistant steels. Increasingly deeper insights on the mechanisms of progress of damage in materials in general and cavitation of heat resistant steels in particular are being facilitated by the application of the destructive 3D techniques such as serial sectioning and the recently developed concept of Correlative Tomography. These developments in field of 3D characterisation of materials and its application to provide new mechanistic insights on the creep cavitation behaviour has important implications for residual life assessment methods. A critical summary presented in the present review of the various methods used to estimate creep life shows that these existing methods clearly falls short of describing the real behaviour of creep cavitation in heat resistant steels, especially at low stress. This lack of understanding has led to the empiricisms in the formulation of parameters to estimate constitutive relationships and an over-simplification of the phenomenological relationships that attempts to describe creep behaviour of heat resistant steels. The range of information from the application of tomographic and other 3D techniques has been largely subjected to mechanistic interpretations. The critical review makes the case that in light of exemplary in-sights on the way in which creep damage progresses in materials, obtained from the application of 3D techniques the use of both the understanding of creep cavitation phenomenon and its quantification can be extended to provide a robust estimate of residual life of heat resistant steels using tomographic technique. In order to realise this two broad areas of research are required – one to develop material constitutive relationships that explicitly uses the cavitation damage parameters to compute creep life and end of life criterion for estimation of residual life, and second is to evolve protocols consisting of 3D techniques with micro-tomography as being central to the convergence of techniques that permits the damage characterisation from reasonably large volumes of material. This will ensure that the damage data is statistically robust and representative of the component exposed to creep degradation. In order to realise this potential, developments in destructive 3D techniques, and computational techniques that can concurrently handle image based modelling techniques with conventional tools such as FEM will be required. These will be dealt in detail in the forthcoming papers.

Acknowledgements

CG thanks JASRI for the award of the beamtimes 2011B1164 and 2012A1049 and all the relevant staff of SPring-8 for support during the experiments that were responsible to provide familiarisation with the versatile capabilities of the micro-tomography technique and enabled the conceptualisation of the critical review proposing the application of tomography for residual life assessment of heat resistant steel components undergoing creep failure. CG also thanks the Director Materials Group, Bhabha Atomic Research Centre, Mumbai, India for support during the preparation of the manuscript.

References

1. R. W. Evans and B. Wilshire: 'Creep of Metals and alloys', 1985, London, Institute of Metals .
2. R. Vishwanathan: 'Damage mechanisms and life assessment of high temperature components', 1989, Ohio, ASM International
3. R. L. Klueh and D. R. Harries: 'Highchromium ferritic and martensitic steels for nuclear applications', 2001, Philadelphia American society for testing and Material.
4. F. Abe:' Bainitic and Martensitic creep resistant steels', Curr. Opinion Solid State Mater. Sci. 2004 8 305 – 339.
5. M. Taneike, F. Abe and K. Sawada: 'Creep strengthening of steels at high temperatures using nano-sized carbo-nitride dispersions' Nature 2003 424 294-296.
6. F. Abe, S. Nakazawa, H. Araki and T. Noda:' The role of microstructural instability on creep behavior of low radio-activation martensitic 9Cr-2W steel', Metall. Trans 1992 23A 469-477.
7. V. Vodarek and A. Strang:' Compositional changes in minor phases present in 12CrMoVNb steels during thermal exposure at 550°C and 600°C Mater. Sci. Technol. 2000 16 1207-1213.
8. G. Eggeler:'The effect of long term creep on particle coarsening in tempered martensitic ferritic steels' Acta. Metall. 1989 37, 3225-3234.
9. M. E. Kassner and T. A. Hayes: 'Creep Cavitation in Metals' Int. Jour. Plast. 2003 19 1715-1748.
10. K. –H. Mayer and F. Masuyama: 'The development of creep resistant steels' in creep Resistant Steels (eds. F. Abe, T. U. Kern, R. Vishwanathan) 15-77; 2008 Woodhead Publishing Ltd. And CRC Press Boca Raton FL 33487 USA.

11. J. Hald: ’ Microstructure and long term creep properties of 9-12%Cr Steels’, Int. Jour. Press. Vess. Pip., 2008 85 30 -37.
12. J. Francis, A. Mazur, H.K.D.H. Bhadesia:’ Review of type IV cracking in ferritic power plant steels’, Mater. Sci. technol. 2006, 22 1387-1395.
13. F. Abe:’ Metallurgy for long term stabilisation of ferrictic steels for thick section boiler components in USC power plant at 650°C, Proc 8thLeighe conference on :Materials for advanced power engineering 2006 leigh Belgium 2006 965- 980.
14. T. Horiuchi, M. Igarshi, and F. Abe:’ Improved utilization of added B in 9 Cr heat resistant steels containing W’, ISIJ Int. 2002 42 567-71.
15. M. Igarshi:’ Alloy design philosophy of creep resistant steels’, in creep Resistant Steels (eds. F. Abe, T. U. Kern, R. Vishwanathan) 539-572; 2008 Woodhead Publishing Ltd. And CRC Press Boca Raton FL 33487 USA.
16. J. Lin, Y. Liu and T. A. Dean:’ A review on damage mechanisms models and calibration methods under various deformation conditions’, Int. J. Damage Mech. 2005 14 299-319.
17. R. Vishwanathan and R. Tilley”’ Creep damage – Industry needs and future research and development’, in Creep Resistant Steels (eds. F. Abe, T. U. Kern, R. Vishwanathan) 637-666; 2008 Woodhead Publishing Ltd. And CRC Press Boca Raton FL 33487 USA.
18. B. Neubauer and V. Wedel:’ Rest life estimation of creeping component by means of replication’, Advances in Life prediction (eds. P. A. Woodford and R. White Head)3017-324 1983 ASME, New York.
19. U. Messerscmidt, M. Bartsch, C. Dietzsch, R. Agamenone, C. Gupta, and W. Blum, Unpublished research.
20. H. Chilukuru, on the microstructural basis of creep strength and creep-fatigue interaction in 9-12% Cr steels for application in power plants, PhD thesis University of Erlangen – Nurnberg Erlangen Germany 2007.
21. W. Blum:’ Mechanisms of creep deformation in steel’, in Creep resistant steels (eds. F. Abe, T. U. Kern, R. Vishwanathan.) 365-401, 2008 Woodhead publishing and CRC Press Boca Raton FL 33487 USA.
22. S. R. Stock:’ Micro-computed Tomography: Methodology and Applications ‘, 2009 CRC press Boca Raton.
23. S. R. Stock:’ Recent advances in X-ray micro-tomography applied to materials’, Inter. Mater. Rev. 2008 53 129-181.

24. J. Baruchel, J. –Y. Buffiere, E. Maire, P. Merle and G. Piex:' X-ray tomography in material science ', 2000 Paris Hermes Science.
25. E. Maire, P. J. Withers: Quantitative Tomography', Inter. Mater. Rev. 2014 59 1-43.
26. A Steuwer, L. Edwards, S. Pratihar, S. Ganguly, M. Peel, M. E. Fitzpatrick, T. J. Marrow, P. J. Withers, I. Sinclair, K. D. Singh, N. Gao, T. Buslaps, J. –Y. Buffiere, 'In situ analysis off cracks in structural materials using synchrotron X-ray tomography and diffraction' Nucl. Instru. Meth. Phys. Res B 246 2006 217-225.
27. B. F. Dyson:' Creep and fracture of metals: mechanisms and mechanics" Rev. Phys. Appl. 1988 23 605-613.
28. C. Gupta, H. Toda, C. Schlacher, Y. Adachi, P. Mayr, C. Sommitsch, K. Uesugi, Y. Suzuki, A. Takeuchi, M. Kobayashi:' A study of Creep cavitation behaviour in tempered martensitic steel using synchrotron micro-tomography and serial sectioning techniques." Mater. Sci. Eng. 2103 A564 525-538.
29. Connolly, B. J., D. A. Horner, S. J. Fox, A. J. Davenport, C. Padovani, S. Zhou, A. Turnbull et al. "X-ray microtomography studies of localised corrosion and transitions to stress corrosion cracking." Materials science and technology 22, no. 9 (2006): 1076-1085.
30. C. Gupta, H. Toda, T. Fujioka, M. Kobayashi, K. Uesugi, A. Takeuchi, Y. Suzuki: " Micro-pore development phenomenon in hydrogen pre-charged aluminium alloy studied using synchrotron X-ray micro-tomography", Appl. Phys. Lett. 2013 103 171902- 1-4.
31. J. –Y Buffiere, E. Maire, P. Cloetens, G. Lormand , R. Fougres:' Characterisation of internal damage in a MMC_P using X-ray synchrotron phase contrast microtomography', Acta. Mater., 1999 47 1613-1625.
32. A. Guvenilir, T.M. Breunig, J. H. Kinney and S. r. Stock:' Direct observation of crack opening as a function of applied load in the interior of a notched tensile sample of Al-Li 2090', Acta. Mater. 1997 45 1977-1987.
33. A. Guvelinir and S. R. Stock:' High resolution computed tomography and its implications for fatigue crack closure modelling', Fatigue Fract. Mater. Struct. 1998 21 439-450.
34. A Guvelinir, T. M. Bruning, J. H. Kinney and S. R. Stock:' New direct observations of crack closure processes in Al-Li 2090 T8E41', Phil. Trans. Roy. Soc. (Lond) 1999 357 2755-2775.

35. H. Toda, I. Sinclair, J. –Y. Buffiere, E. Maire, T.Connolly, M. Joyce, K. H. Khor, P. Gregson:' Assessment of fatigue crack closure phenomenon in damage tolerant aluminum alloy by in-situ high resolution synchrotron X-ray micro-tomography', Philos. Mag. 2003, 83 2429 – 2448.
36. S. F. Nielsen, F. Beckmann, H. F. Poulsen, J. A Wert"Measurements of components of plastic displacement gradients in three dimensions ', Mater. Sci. Eng. 2004 A387-389 336-338.
37. S. F. Nielsen, H. F. Poulsen, F. Beckmann, C. Thorning, J. A. Wert: 'Measurements of plastic displacement gradient components in three dimensions using marker particles and synchrotron microtomography", Acta Mater. 2003 51 2407-2415.
38. M. Kobayashi, H. Toda, Y. Kawai, T. Ohgaki, K. Uesugi, D. S. Wilkinson, T. Kobayashi, Y. Aoki, M. Nakazawa:' High density three dimensional mapping of internal strains by Tracking microstructural features', Acta. Mater. 2008 56 2167-2181.
39. A. Pyzalla, B. Camin, T. Buslaps, M. Di. Michiel, H. Kaminski, A. Kottar, A. Pernack, W. Reimers:' Simultaneous tomography and diffraction analysis of creep damage", Science 2005 308 92-95.
40. F. Sket, K Dzieciol, A. Issac, A Borbely, A. R. Pyzalla:' Tomographic method for evaluation of apparent activation energy of steady state creep', Mat. Sci. Eng. 2010 A257 2112-2120.
41. D. Kurumulu, E. J. Payton, M. L. Young, M. Schöbel, G. Requena, G. Eggler: ' High temperature strength and damage evolution in short fiber reinforced aluminium alloys studied by miniature creep testing and synchrotron microtomography', Acta. Mater. 2012 60 67-78.
42. A. Issac, F. Sket, W. Reimers, B. Camin, G. Sauthoff, A. R. Pyzalla:' In-situ 3D quantification of the evolution of creep cavity size, shape and spatial orientation using synchrotron tomography', Mater. Sci. Eng. A 478 108-118.
43. K. Dzieciol, A. Borbely, F. Sket, A. Issac, M. DiMiciel, P. Cloetens, T. Buslaps, A. R. Pyzalla:' Void growth in copper during high temperature power law creep', Acta. Mater. 2011 59 671-677.
44. Z. Asghar, G. Requena, H. P. Degischer, P. Cloetens:' Three dimensional study of Ni Aluminide in an AlSil2 alloy by means of light optical and synchrotron microtomography', Acta. Materialia. 2009 57 4125-4132.

45. G. Requena, P. Degischer, E. D. Marks, E. Boller:' Microtomography study of the evolution of microstructure during creep of an AlSil2CuMgNi alloy reinforced with Al_2O_3 short fibers', Mat. Sci. Eng. 2008 487A 99-107.
46. K. E. Yazie, J. J. Williams, N.C. Philips, F. De Carlo, N. Chawla:'Multiscale microstructural characterisation of Sn-rich alloys by three dimensional (3D) X-ray synchrotron microtomography and focussed ion beam (FIB) tomography', Mater. Charact. 292 70 33-41.
47. Ke-shencheong, K. J. Stevens, Y, Suzuki, K. Uesugi, A. Takeuchi:'The effects if microstructure on creep behaviour – A study through synchrotron microtomography', Mat. Sci. Eng. 2009 A 513-514 222-227.
48. F. Sket, K. Dzieciol, A. Borbely, A. R. Kaysser – Pyzalla, K. Maile, R. Scheck :'Microtomographic investigation of damage in E911 steel after long term creep', Mat. Sci. Eng. 2010 528A 103-111.
49. F. Sket, A. Issac, K. Dzieciol, G. Sauthhoff, A. Borbely, A. R. Pyzalla:' Insitu tomographic investigation of brass during high temperature creep', Scripta. Mater. 2008 59 558-561.
50. A. A. Wahab, M.V. Kral:"3D Analysis of Creep voids in hydrogen reformer tubes", Mat. Sci. Eng. 2005 A412 222-229.
51. A. A. Wahab, C. R. Hutchinson, M. V. Kral:" A three- dimensional charcaterisation of Creep void formation in hydrogen reformer tubes", Scripta.Mater. 2006 55 69 - 73.
52. M. D. Uchic: "Serial sectioning methods for generating 3D characterisation data of grain and precipitate scale microstructures", in Compuational Methods for Microstructure - Property Relationships (eds. S. Ghosh and D. Dimiduk) DOI 10.1007/978-1-4419-0643-4, Springer USA, 31-57.
53. H. Toda, K. Uesugi, A. Takeuchi, K. Minami, M. Kobayashi, T. Kobayashi:" Three-dimensional observation of nanoscopic precipitates in an aluminium lloy by microtomography with Fresnel zone plate optics", Appl. Phys. Lett. 2006 89 143112.
54. E. L. Robinson: 'Effect of temperature variation on the creep strength of steels', Trans ASME 1938 160 253-259.
55. R. V. Hart:' Concept of area - modified stress for life fraction summations during creep', Metal. Technol. 1977 4 447-448.
56. R. V. Hart:' Assessment of remaining creep life using accelerated stress rupture tests', Metal. Technol. 1976 3 1-7.

57. R. V. Hart:’ Comparison of biaxial and uni-axial longtitudinal rupture tests for determination of residual creep life of ferritic heat exchanger tubing ‘, Metal technol. 1976 4 442-446.
58. H. E. Evans: " mechanisms of creep Fracture", 1984, Elsevier Applied Science Publication, Essex, UK.
59. H. K. D. H. Bhadeshia, A. Strang, D. J. Gooch:" Ferritic power plant steels: Remanent life assessment and approach to equilibrium", Inter. Mater. Rev. 1998 43 45-69.
60. F. Philips:’ the slow stretch in india rubber glass and metal wire subjected to constant pull’, Phil Mag 1905 9 513-520.
61. A. Graham and K. F. A Walles:’ Relation between long and short time properties of commercial alloy’, JISI 1955 179 105-120.
62. P. G. McVetty:’ Factors affecting the choice of working stresses for high temperature service’, 1933 Trans ASME 55 99-109.
63. J. B. Conway and M. J. Mullikin:’ An evaluation of various first stage creep equations’, 1962 in Proc AIME conference Detroit Michigan.
64. F. N. Norton:’ The creep of steel at high temperature’, 1929 McGraw Hill book Inc NY USA.
65. A. Nadai:’ The influence of time upon creep, The hyperbolic sine creep law’, in Stephen Timoshenko Anniversary volume, 1938 Macmillian, New York..
66. B. K. Choudhury and E. I. Smauel:’ Creep behavior of modified 9-Cr1Mo ferritic steel’, Jour. Nucl. Mat. 2011 412 82-89.
67. E. I. Samuel and B. K. Choudhary, D. P. R. Palaparti, M. D. Mathew:’ Creep deformation and rupture behaviour of P92 Steel at 923K’, Procedia Eng. 2013 55 64-69.
68. D. P. R. Palaparti, E. I. Samuel, B. K. Choudhary, M. D. Mathew:’ Creep properties of Grade 91 steel steam generator tube at 923K’, Procedia Eng. 2013 55 70-77.
69. B. Wishire, P. J. Scharning: Design data prediction for Grade P92 steel', Proc Creep8: 8th international conf. on creep and fatigue at elevated temperatures, 22-26 July 2007, San Antonio USA.
70. M. W. Spindler, S. L. Spindler: Creep deformation, rupture and ductility of Esshete 1250 weld metal", Mater. Sci. Technol. 2014 30 17-23.
71. M. E. Kassner and M. –T. Perez Prado:’ Five power law creep in single phase metals and alloys’ Prog. Mat. Sci. 2000 1-102.

72. G. Dimmler, P. Weinert, P. Cerjack:'Extrapolation of short term creep data – The potential risk of extrapolation ' Int. Press. Vess. Pip. 2008 85 55-60.
73. P. Yavari and T. G. Langdon :' An examination of breakdown in creep by viscous glide in solid solution alloys at high stress levels" Acta. Mater. 1982 30 2181 – 2190.
74. Y. X. Chen, W. Yan, W. Wang, Y. Y. Shan, and K. Yang:' Constitutive equation of the minimum creep rate for 9%Cr heat resistant steel' Mat. Sci. Eng. 2012 A534 649-653.
75. H. J. McQueen and N.D. Ryan:' Constitutive analysis of hot working', Mat. Sci. Eng. A322 2002 43-63.
76. F. Garofalo:' Fundamentals of creep and creep rupture in metals', 1965 McMillan NY USA.
77. B. Cane and J. A. William:'Remaining life prediction of high temperature materials ', Int. Mater. Rev. 1987 32 241-262.
78. P. W. Davies, W. J. Evans, K. R. Williams and B. Wilshire:' An equation to represent strain/time relationships during high temperature creep', Scripta. Metall. 1969 3 671-674.
79. R. W. Evans and B. Wilshire:' Creep of metals and alloys", 1985 Institute of metals London.
80. R. Motera:' High temperature time dependent allowable stress and isochronous curves of an austenitic MnCr steel", Jour. Nucl. Mat. 1988 155-157 639-643.
81. A. K. Koul and R. Castillo:' A critical assessment of the θ projection concept for creep life prediction of nickel based super – alloy' Mat. Sci. Eng. 1991 A138 213-219.
82. H. Wolf, M. D. Mathews S. L. Mannan and P. Rodriguez:' Prediction of creep parameters of type 316 stainless steel under service conditions using the θ projection concept', Mat. Sci. Eng. 1992 A159 199-204.
83. C. M. Omprakash, A. Kumar, B. Srivathsa, D.V.V.Satyanarayana:'Prediction of Creep Curves of High temperature alloys using θ - Projection Concept', Procedia Eng. 2013 55 756-759.
84. A Loghman, M. A. Wahab:' Creep Damage simulation of thick walled tubes using the θ Projection concept ', Int. J. Press. Pip. 1996 67 105-111.
85. S. Fujibayashi:' Creep behavior leading to Type IV cracking for service exposed 2.25Cr-0.5Mo steel welds', Eng. Fract. Mech. 2007, 74 932-946..
86. R. N. Ghosh:' Creep life prediction of engineering components: Problems and prospects', 2103 ProcediaEngineering 55 599-606.

87. F. Krumphals, B. Reggiani, L. Donati, T. Wlanis, C. Sommitsch: ‘Deformation behaviour of ferritic hot – work tool steel with respect to the microstructure’ Comp.Mater.Sc. 52 (2012) 40-45
88. F. A. Leckie and H. R. Hayhurst:’ Constitutive equations for creep rupture’, Acta Metall. 1977 25 1059-1070.
89. R. K. Penny and D. L. Marriot:’ Design for Creep, 1971, McGraw Hill New York.
90. F. Krumphals., T. Wlanis, R. Sievert, V. Weiser, C. Sommitsch: ‘Damage analysis of extrusion tools made from austenitic hot work tool steel Böhler W750’, Comp.Mater.Sc. 50 (2011) 1250-1255.
91. L. M. Kachanov:’ Time to failure under creep conditions’, Izv. Akad. Navk SSR OtdTeckNauck, 1958 8 26 – 31.
92. L. M. Kachanov:’ Introduction to continuum damage mechanics’, Kluwer Academic Dordrecht.
93. B. F. Dyson and M. McLean:’Microstructural evolution and its effects on creep performance of high temperature alloy’, 1998 in Microstructural stability of creep resistant alloys for high temperature plant application (ed. A. S. Strang et. al.) IOM London 371-373..
94. B. F. Dyson an D. Mclean:’ Creep of Nimonic 80A in torsion and tension’ Metal . Sci. 1977 11 37 – 45.
95. B. F. Dyson and M. McLean:’Particle coarsening, σ_o and tertiary creep.’,Acta. Metall. 1983 31 17
96. B. F. Dyson and F. A. Leckie:’Physically based modeling of remanant creep life’ Mater. Sci. Eng. 1988 A103 111-114.
97. B. J. Cane:’ Remaining creep life estimation by strain assessment of plant.’, Int. Jour. Press. Vess. Pip 1982 10 11-17.
98. S. Hore and R. N. Ghosh:’ Computer simulation of high temperature creep behaviorof Cr-Mo steel’, Mat. Sci. Eng. 2011 A258 6095-6102.
99. W. Blum, A. Rosen, A. Cegielska, J. L. Martin, " Two Mechnaisms of dislocation motion during Creep", Acta. Metall. 1989 37 2439-2453.
100. M. Meier, W. Blum: " Modelling high temperature Creep of academic and industrial materials using the composite model", Mat. Sci. Eng. 1993 A164 290-294.
101. R. Sedlacek, W. Blum:" Microstructure based constitutive law of plastic deformation" Comp. Mater. Sci. 2002 25 200-206.

102. H. Mughrabi :" Dislocation wall and cell structures and long range internal stresses in deformed metal crystals" Acta. Metall. 1983 31 1367-1379.

103. T. Barkar, J. Agren:" Creep simulaton of 9-12% Cr Steels using the composite model with thermodynamically calculated input", Mat. Sci. Eng. 2005 395A 110-115.

104. T.H. Hyde, W. Sun, J.A. Williams:" Requirements and use of miniature test specimens to provide mechanical and creep properties of materials", Inter. Mater. Rev. 2007 52 213-255.

105. R. C. Thompson, H. K. D. H. Bhadhesia: "Changes in chemical composition of carbides in 2.25Cr-1Mo power plant steel: Part 1"Mater. Sci. Technol. 1994 10 193-204.

106. R. C. Thompson, H. K. D. H. Bhadhesia: "Changes in chemical composition of carbides in 2.25Cr-1Mo power plant steel: Part 2"Mater. Sci. Technol. 1994 10 205-208.

107. D. Lonsdale, P.E.J.Flewitt: "Damage accumulation and microstructural changes occurring during creep of a 21/4% Cr1%Mo steel" Mater. Sci. Engg. 1979 39 217-229.

108. W. Blum, G. Gotz: " Evolution of dislocation structure in martensitic steels: The subgrain size as a sensor for creep strain and residual creep life", Steel Res. 1999 70 274-278.

109. A. Afrouz, M.J.Collins R. Pilkington: "Microstructural examination of 1Cr-O-5Mo steel during creep", Met. Technol., 1983 10 461-463.

110. P. Hofer, H. Cerjack, B. Schaffermak, P. Warbichlet' Quantification of precipitates in advanced creep resistant 9-12% Cr Steels" Steel Research, 69 Steel Res. 1998,343-348.

111. J. D. Parker, J. D. James:" Disk bend creep deformation behaviour in 0.5Cr0.5Mo0.25V low alloy steel" Creep and Fracture of engineering and structures, 1993 651-660.

112. K Miliscka, F. Dobes:" Small punch testing of P91 steel", Int. Jour. Press. Vess.Pip., 2006 83 625-634.

113. B. Ule, R. Sturm, V. Leskovsek:" Effets of test specimen geometry on creep behavior of 12 Cr steel in miniature disk bend tests", Mater. Sci. Technol. 2003 19 1771 - 1776.

114. S. Komazaki, T. Kato, Y. Kohno, H Tanigawa:" Creep property measurements of welded joint of reduced activated ferritic martensitic steel by small punch creep test", Mater. Sci. Eng.A, 2009 510 229-233.

115. F. Dobes, K. Miliscka:" On the Monkman Grant relation for small punch test data", Mater. Sci. Eng.A, 2002 336 245-248.

116. J. Chakrabarty : " A theory of stretch forming over hemispherical punch heads", Int. Jour. Mech. Sci. 1970 12 315-325.

117. T. L. Burnett, S. A. Mcdonald, A. Gholinia, R. Geurts, M. Janus, T. Slater, S. J. Haigh, C. Omek, F. Almuaili, D. L. Engelberg, G. E. Thompson, P. J. Withers:" Correlative Tomography", Sci. Rep. 2014 4 4711 DOI 10.1038/srep04711.

118. L. Renversade, H. Ruoff, K. Maile, F. Sket, A. Borbely:"Microtomographic assessment of damage in P91 and 911 steels after long term creep", Int. J. Mater. Res. (formerly Z. Metallkd) 2014 105 621-627.

119. H. Riedel:" Fracture at high temperature", Springer-Verlag, 1987 Berlin DOI:10.1007/978-3-642-82961-1.

120. F. Sket, K. Dzieciol, A. Borbely, A.R. Kaysser-Pyzalla, K. Maile, R. Scheck:" Microtomographic investigation of damage in E911 steel after long term creep", Mat. Sci. Eng. 2010 A528 103-111.

121. C. Schlacher, T. Pelzmann, C. Beal, C. Sommitsch, C. Gupta, H. Toda, P.Mayr:"Investigation of creep damage in advanced martensitic chromium steel weldments using synchrotron X-ray micro-tomography and EBSD", in Spl issue. Cavitation in Materials : New Insights (eds. C. Gupta et. al.) Mater. Sci. Tech. 2014 this issue DOI: 10.1179/1743284714Y.0000000621.

122. J. D. Landes and J. A. Begeley:' A fracture mechanics approach to creep crack growth" in Mechanics of crack growth pp128-148 ASTM STP 590 American Society for testing and materials (1976).

123. F. Dobes, K. Miliscka: " The relation between minimum creep rate and time to fracture", Met. Sci. 1976 10 382-384.

124. S. I. Lieberman, A. M. Gokhale, S. Tamirisakandala: "Reconstructions of three dimensional microstructures of TiB phase in a powder metallurgy Titanium alloy using montage serial sectioning", Scripta. Mater.55 2006 63 -68.

125. J.-R. Li, L.-L.Yu: Computational simulation of intergranular fracture of polycrystalline materials and size effect", Eng. Fract. Mech. 2005 72 2009-2017.

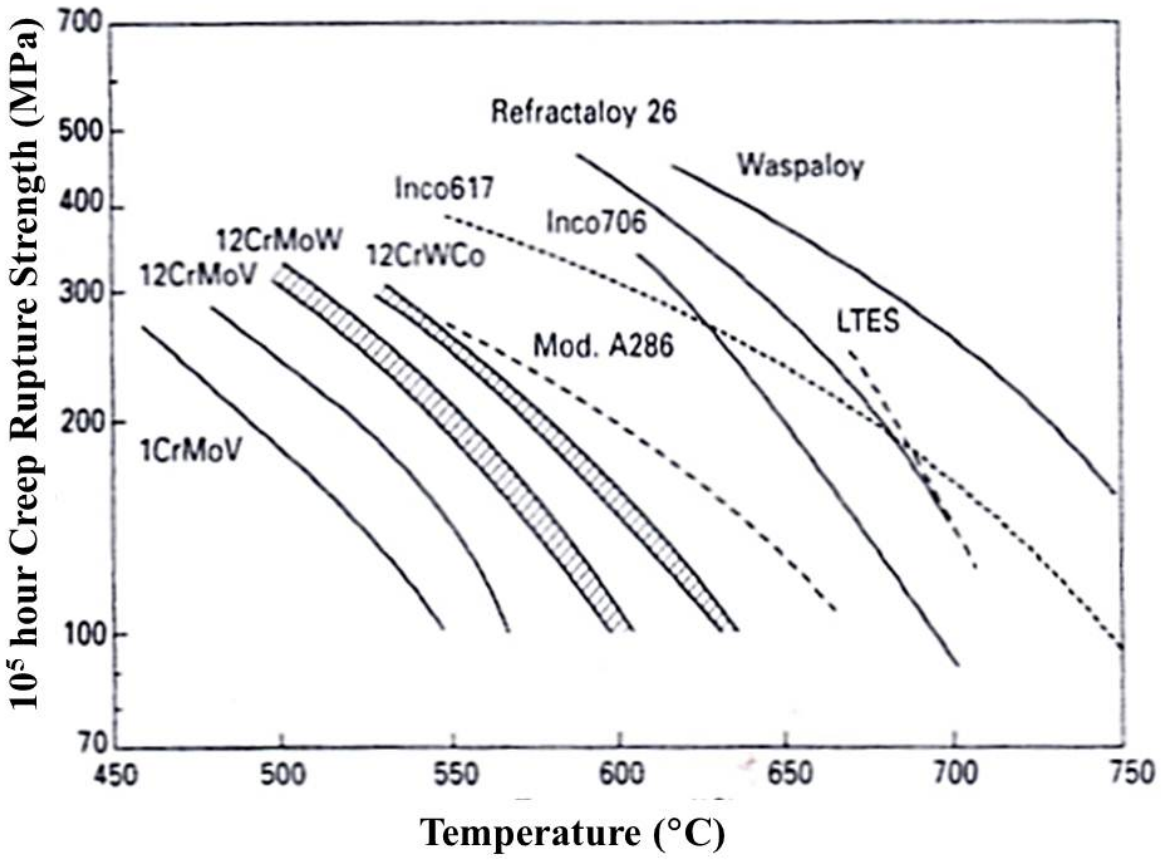

Figure 1: 100 MPa – 10^5 hour creep life of a various classes of heat resistant steels.[10]

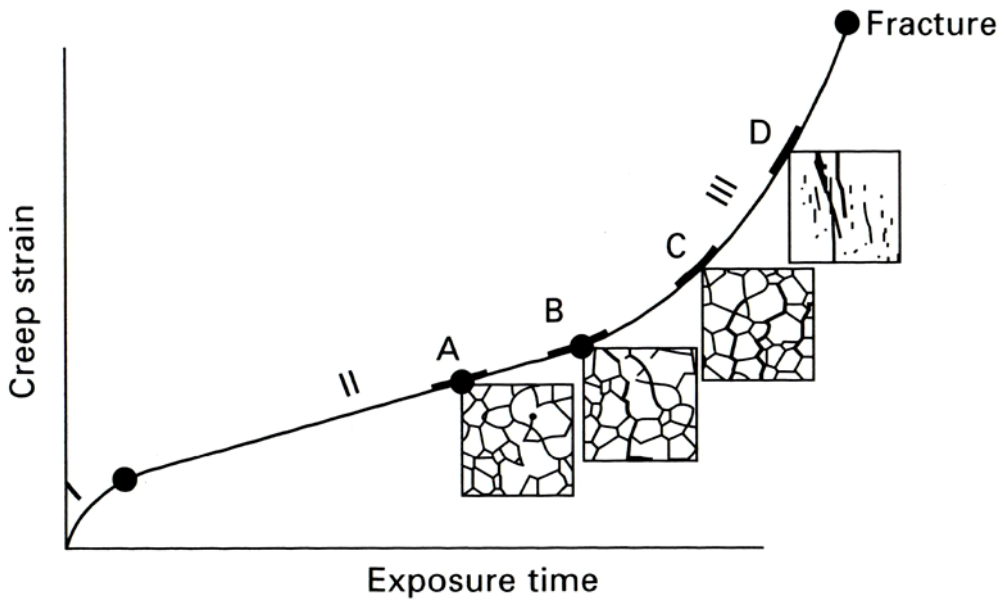

Figure 2:The evolution of cavitation at various stages of the creep life determined from surface replica technique.[18]

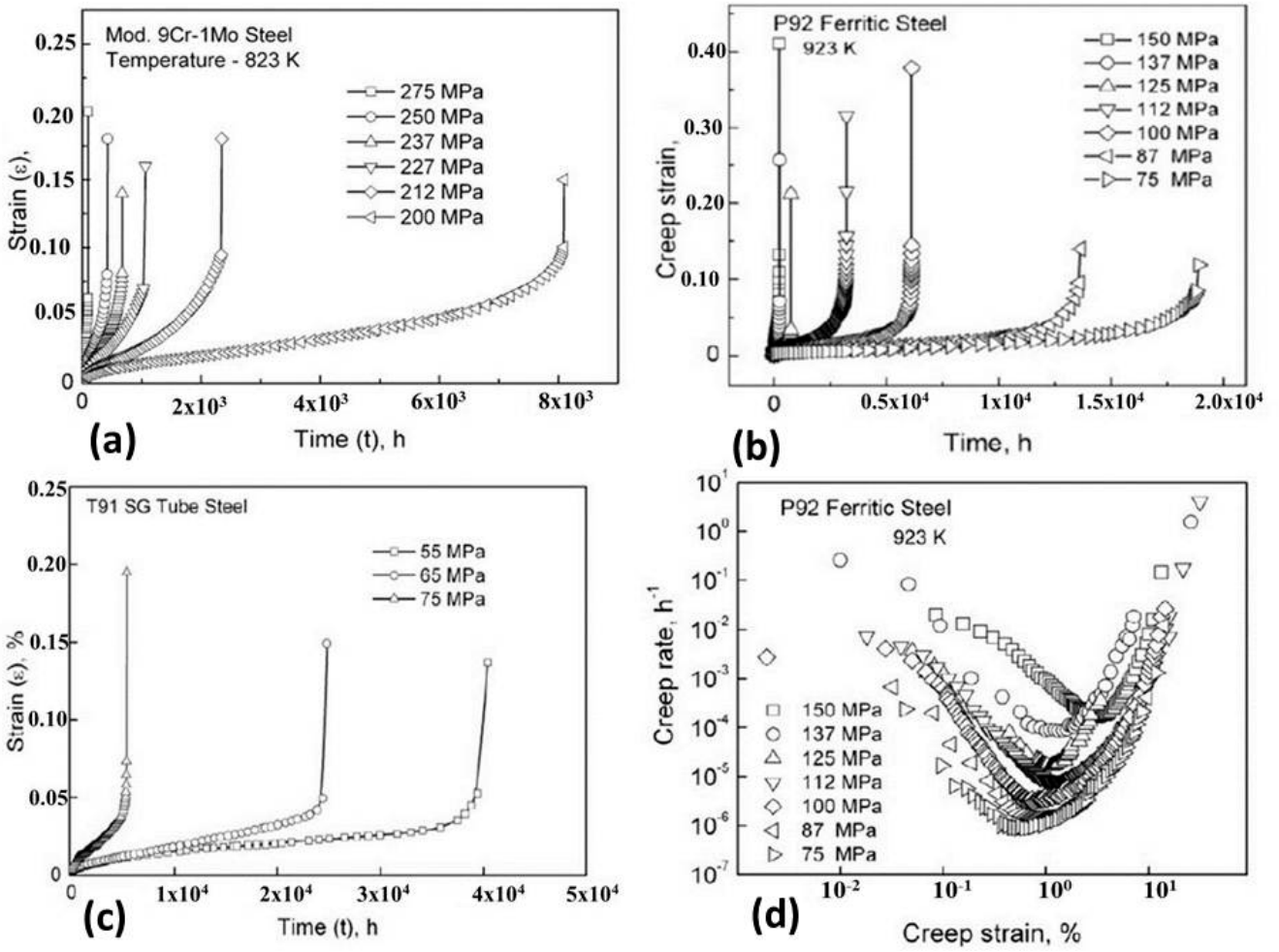

Figure 3:Stress rupture results obtained in modern tempered martensitic steels.[41-43]

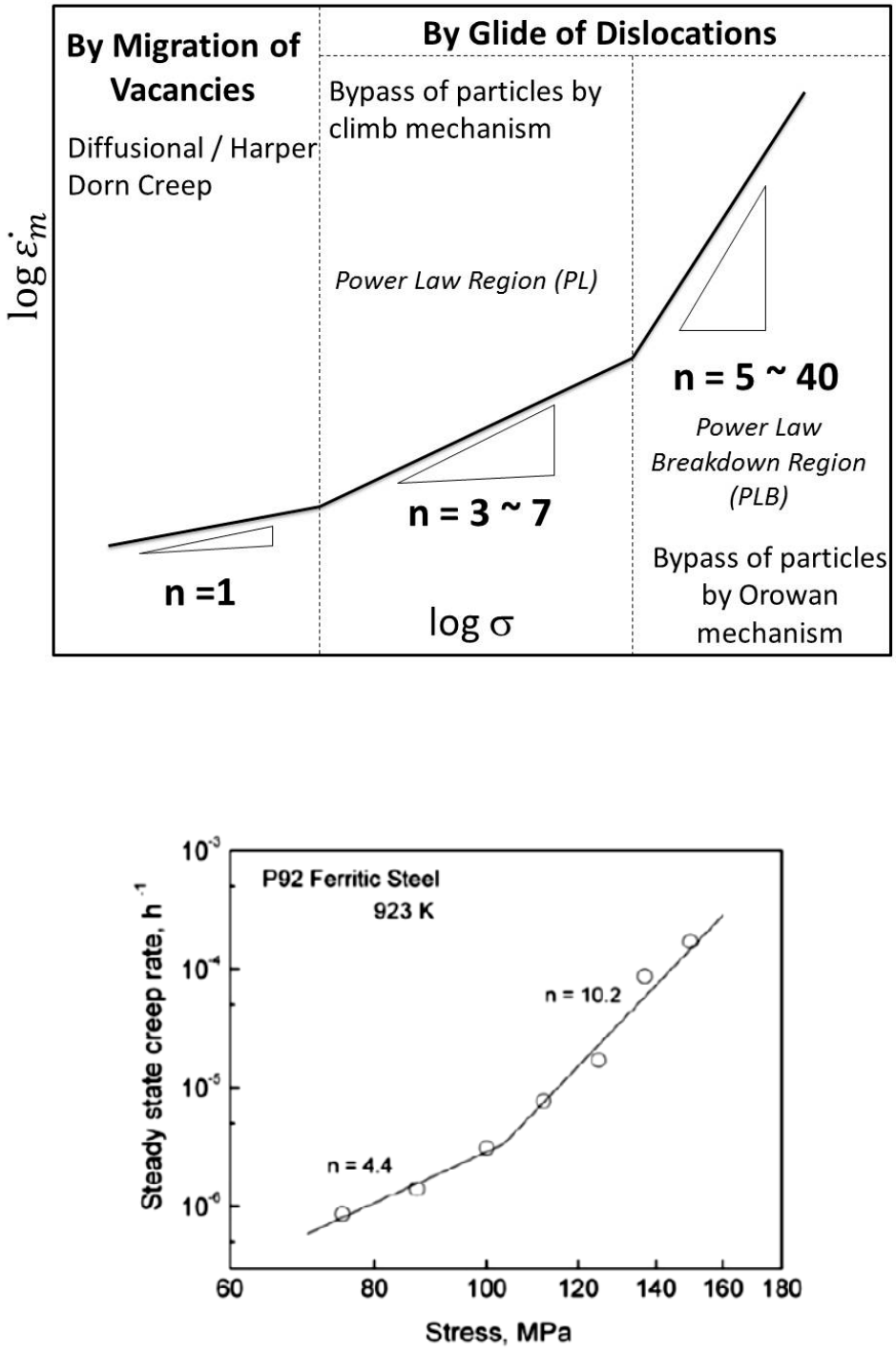

Figure 4: (a) Schematic plot of the regimes of creep distinguished by the stress exponent in tempered martensitic steels and (b) the change in stress exponent with stress for P92 steel at 650°C[42].

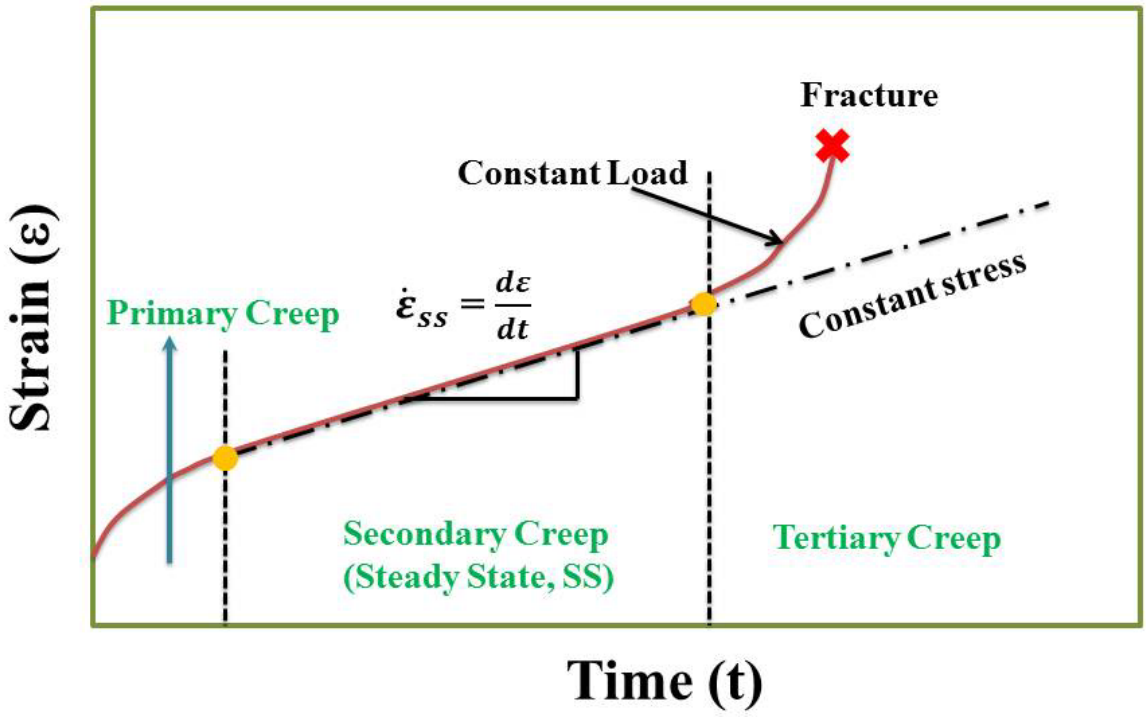

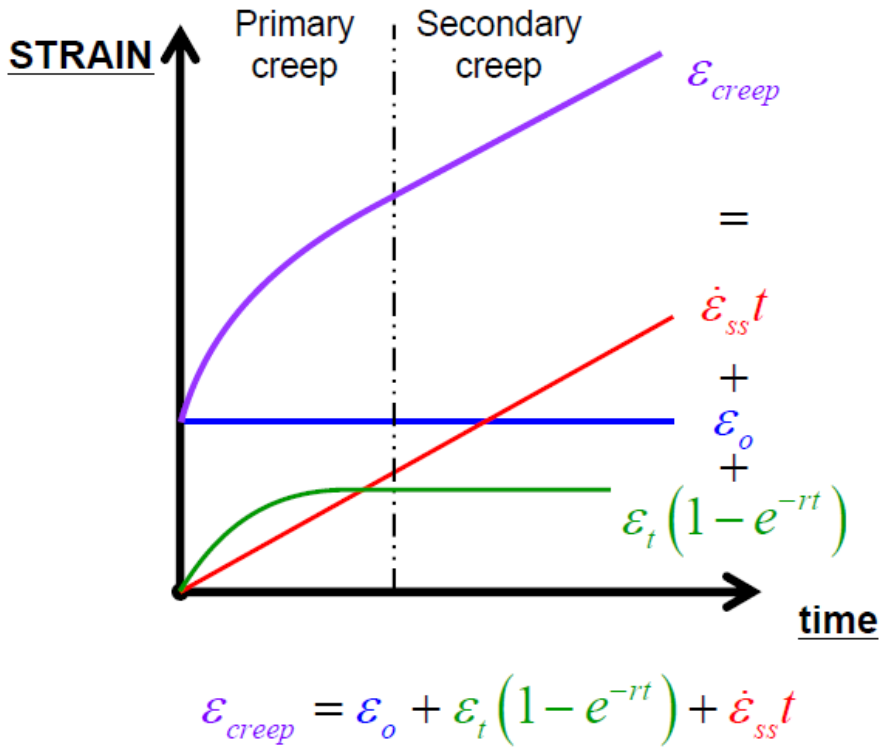

Figure 5: (a) Schematic plot of the strain – time curve from a typical creep test and its fit obtained fromtheGarofaloequation and (b) the decomposition of the Garofalo equation terms as a function of time.

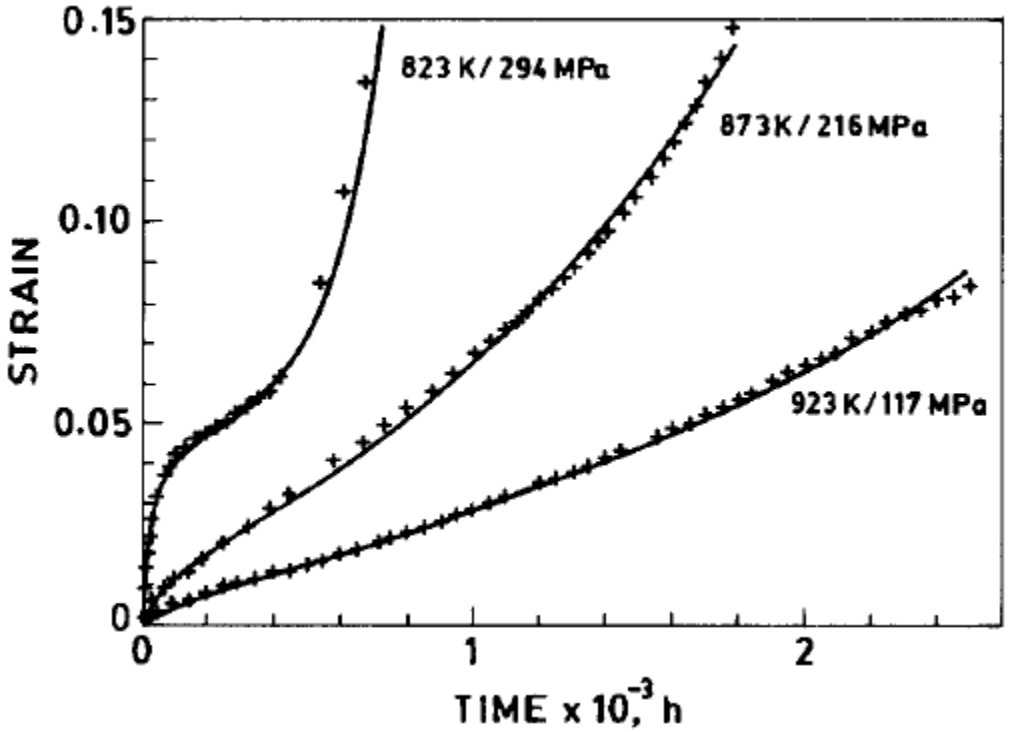

Figure 6:Experimental creep strain – time curves for a 316 stainless steel and their fits using the theta projection equation for various combinations of stresses and temperatures.[57]

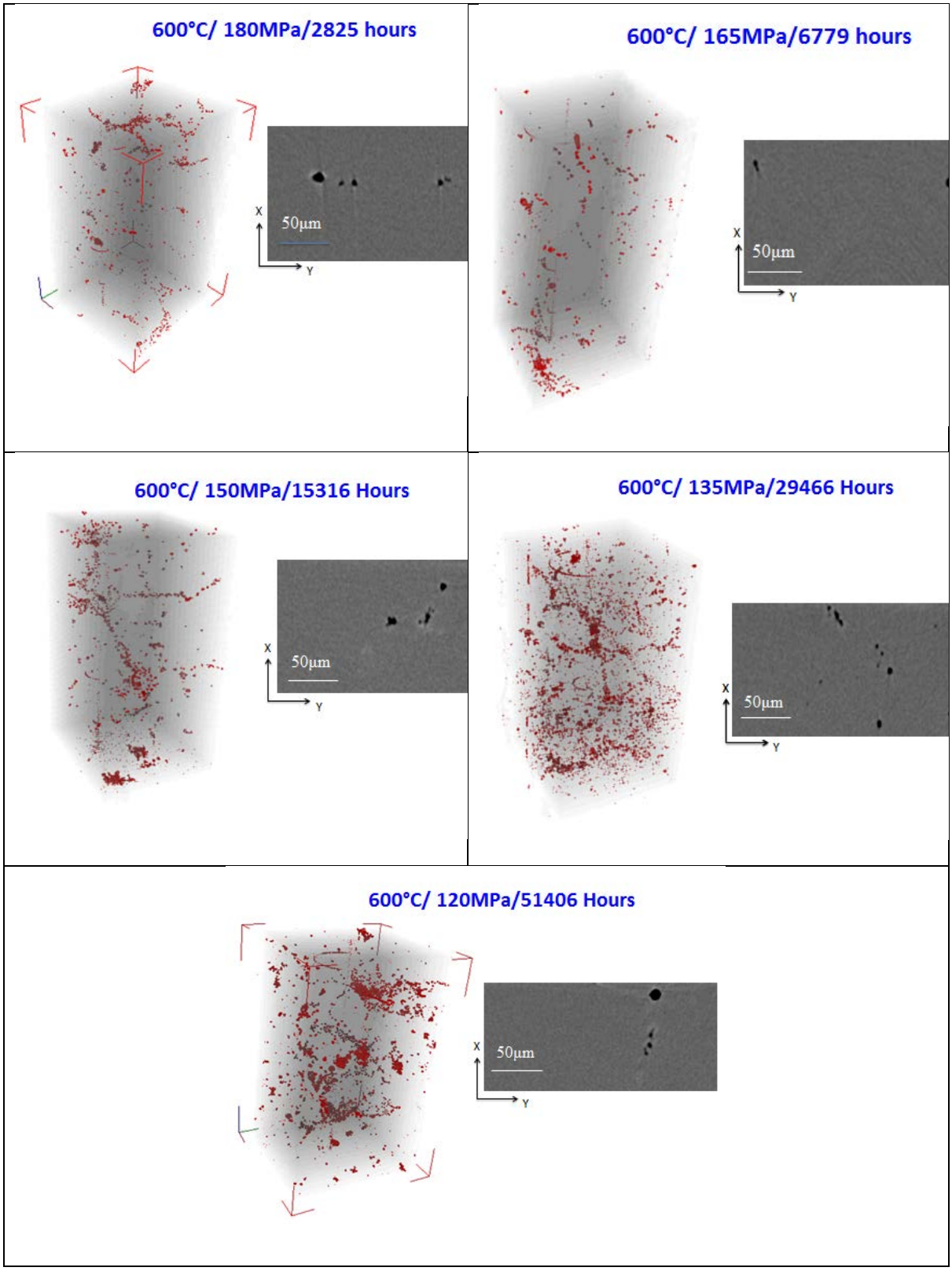

Figure 7: 3D visualization plots of the microtomography datasets extracted from samples crept at 600°C over the stress range 120 – 180 MPa. An extract of the 2D slices for each dataset is shown containing the reconstructed image of creep voids.

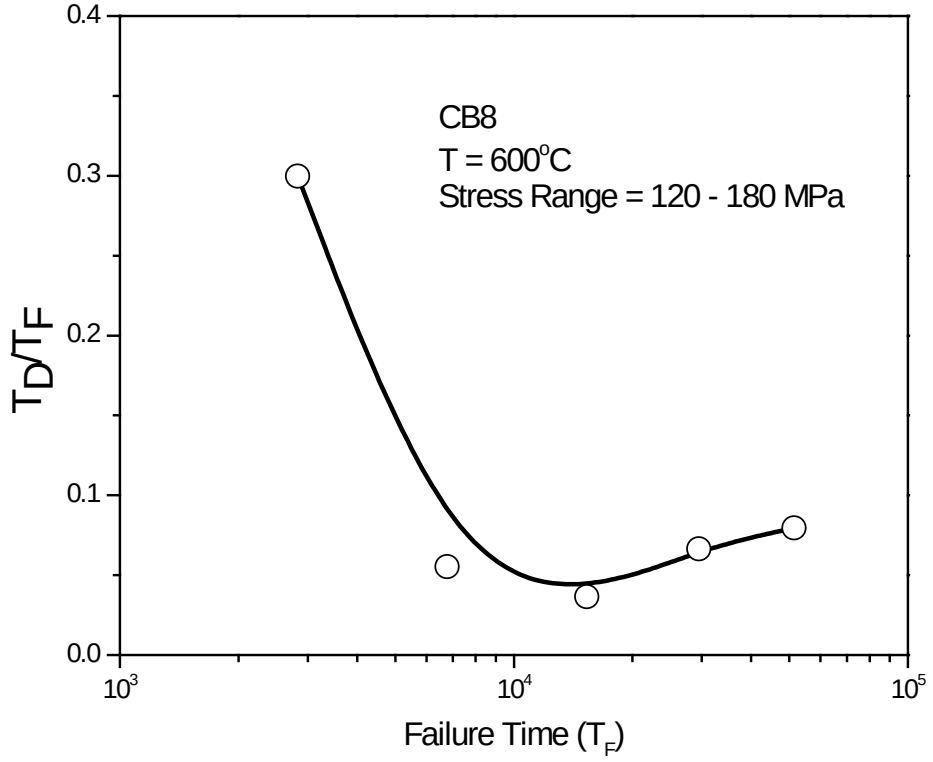

Figure 8:Variation of fraction of creep life spent in the cavitation dominated region with respective failure time over the applied stress range 120 – 180 MPa.

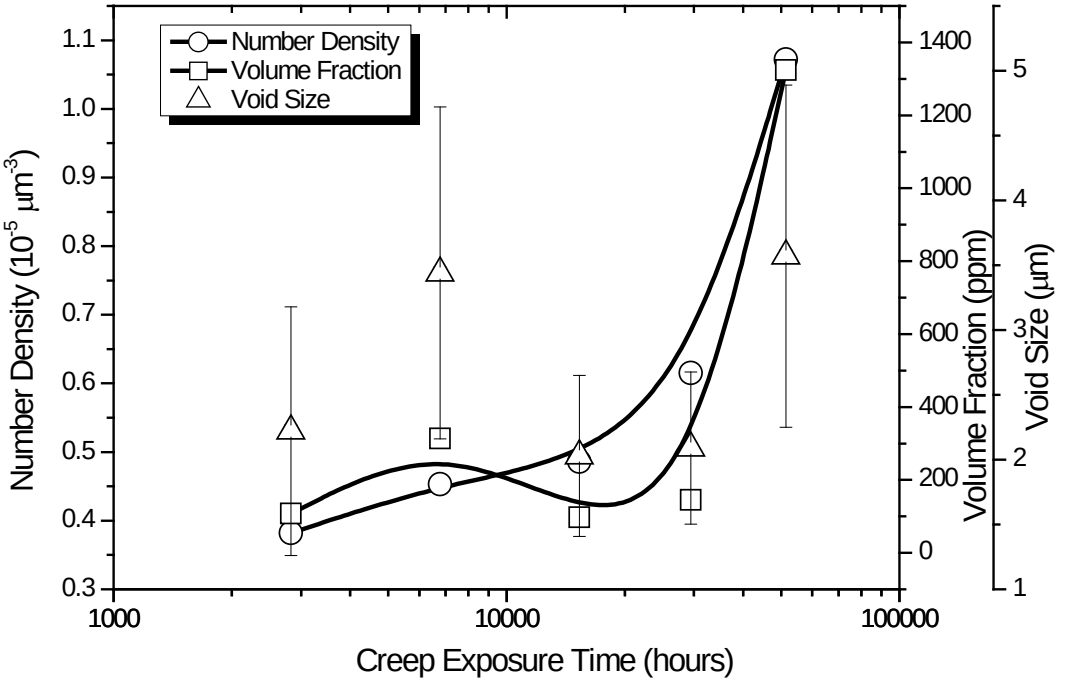

Figure 9:Variation of overall number density, volume fraction and average void size as a function of creep exposure time over the stress range 120 – 180 MPa for CB8.

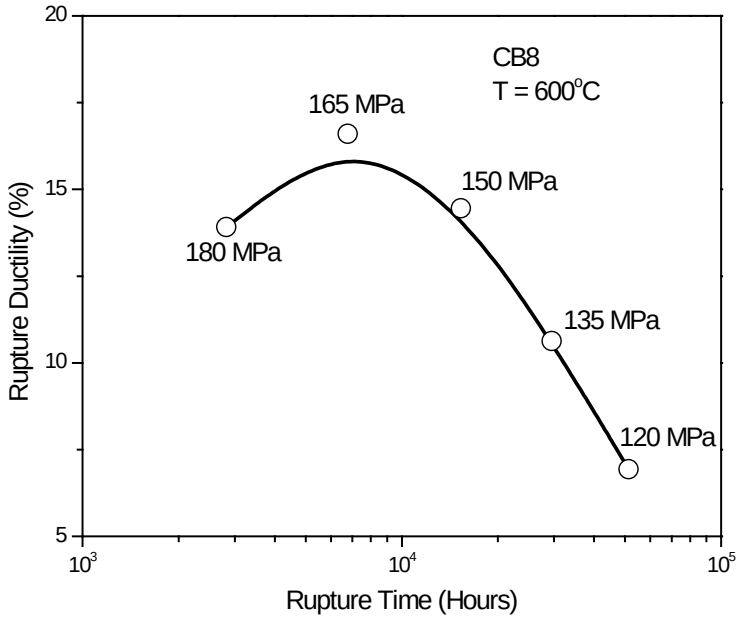

Figure 10:Variation of rupture ductility as a function of creep exposure time over the stress range 120 – 180 MPa for CB8.

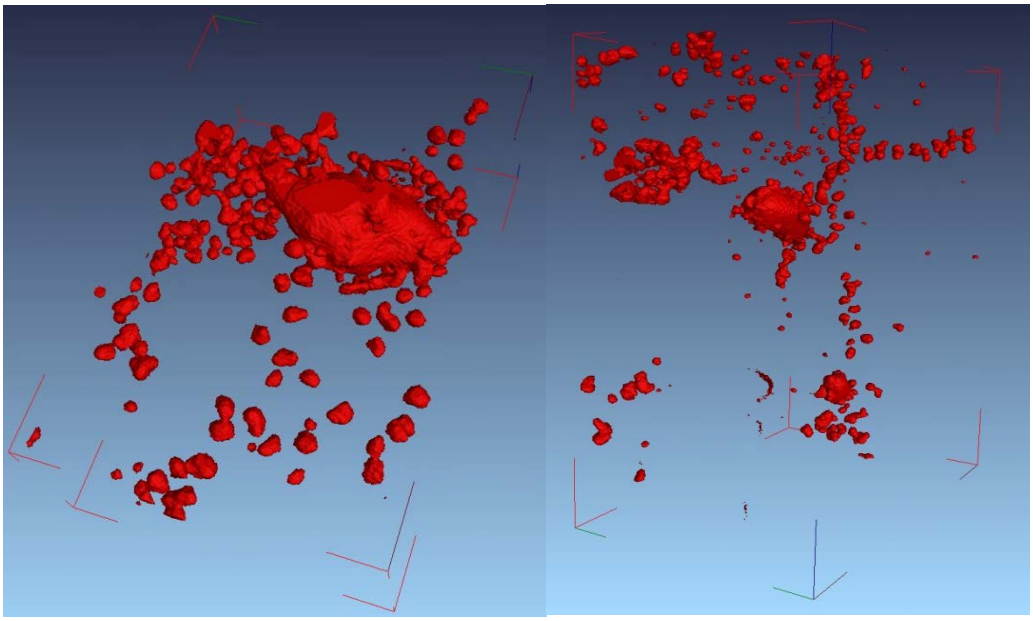

Figure 11: Close up 3D rendering of sub-volumes near to void clusters seen in dataset of a sample crept at 120 MPa revealing the complex morphology of the cavitation.

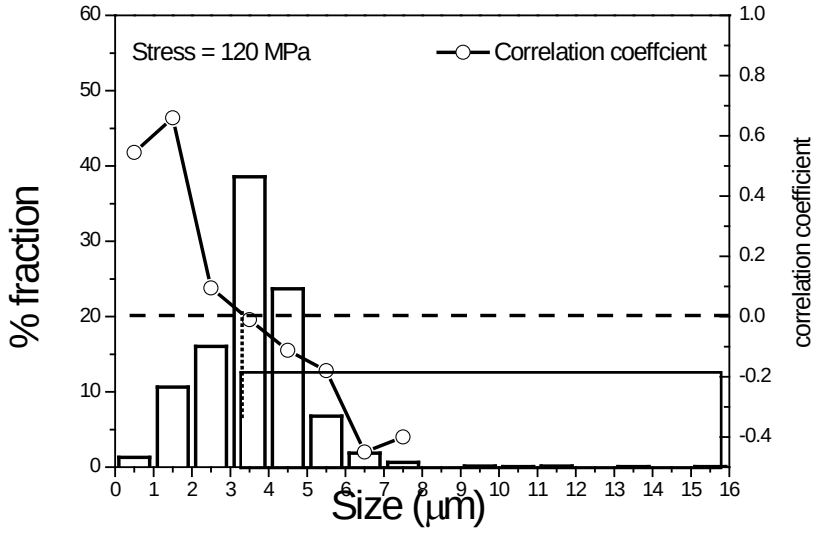

Figure 12:Sizedistribution of the creep voids determined for the dataset of the sample crept at 120 MPa for CB8. The variation of the correlation coefficient of the sphericity of voids with size for each of the size range is shown which serves as a parameter to estimate the coalescence affected fraction (details in C. Gupta et.al.[28])

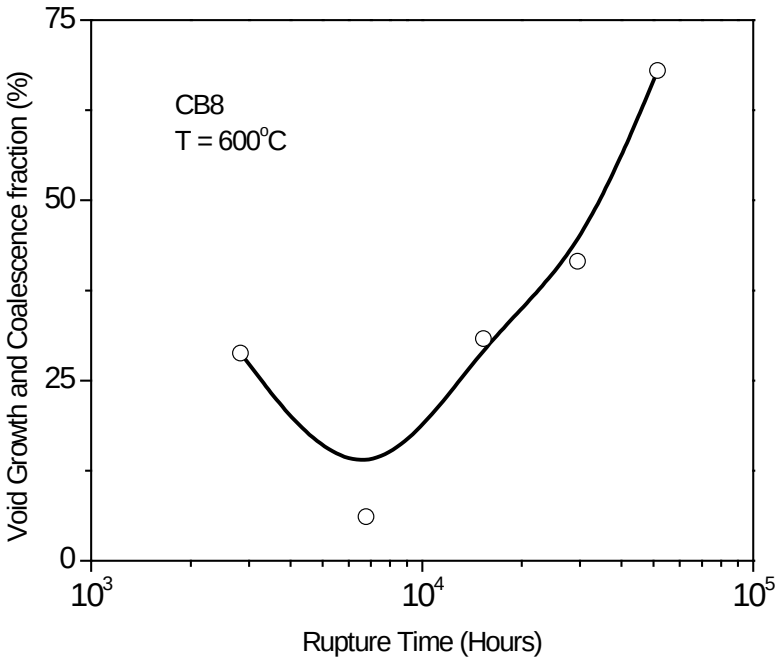

Figure 13: The variation of the coalescence affected fraction of the creep voids as a function of failure time over stress range 120 – 180 MPa.

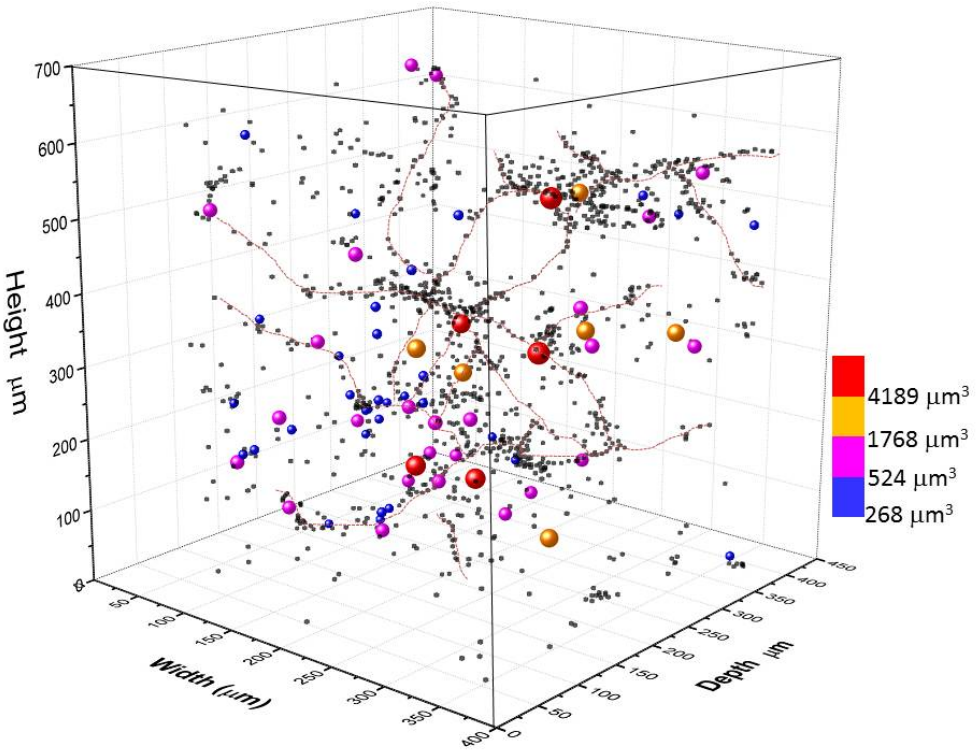

Figure 14: 3D scatter plot showing the proximity of the voids below 268µm^3 to those in having a greater volume in the dataset obtained from a sample crept at 120 MPa.

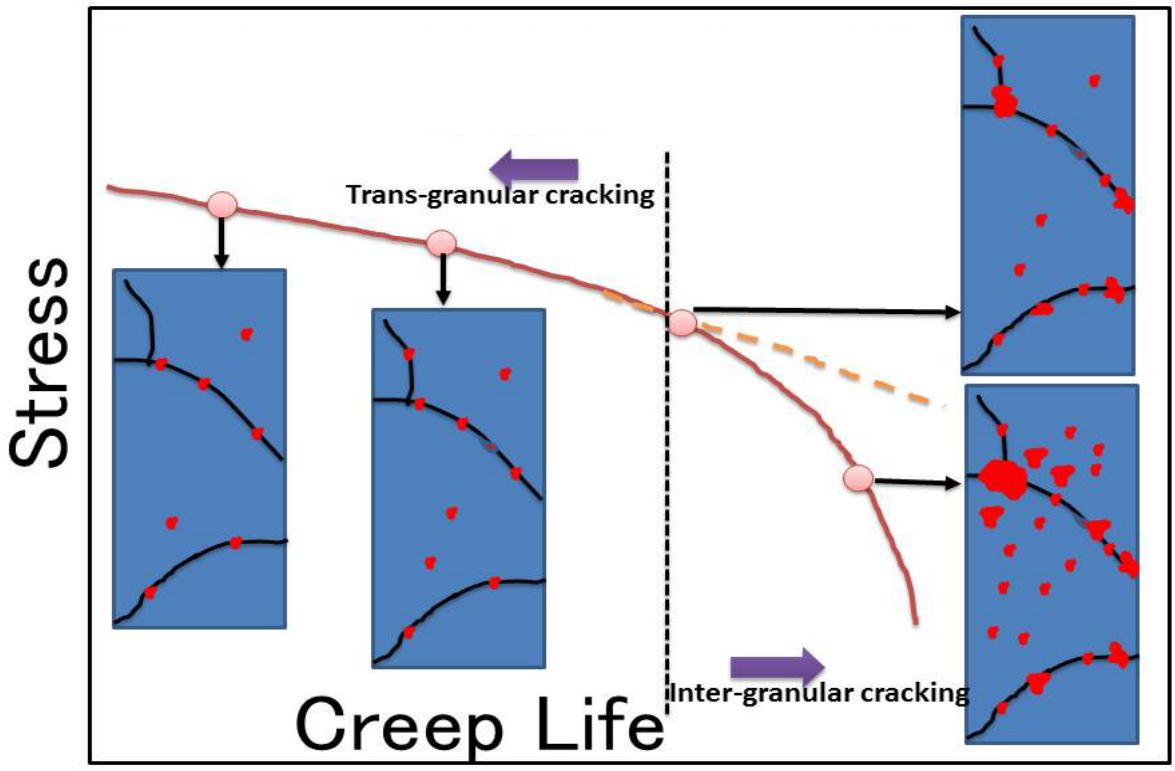

Figure 15: A schematic plot showing the relationship between evolution of cavitation and the decrease in creep life as a function of stress as suggested by the results of CB8[28].

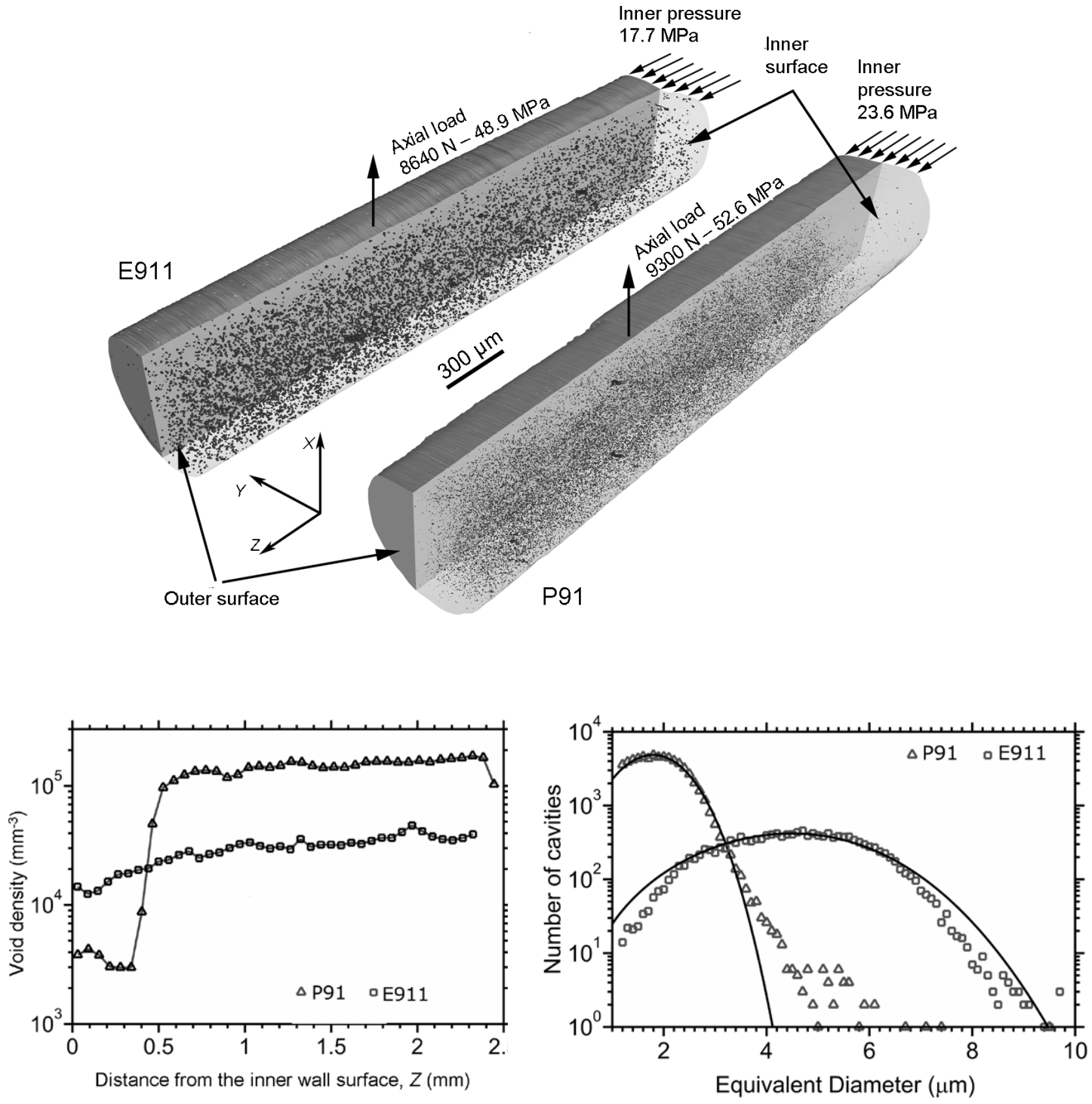

Fig. 16(a) 3D rendering of the cavitation in P91 and E911 steels exposed to creep for 10200 hours and 37,800 hours respectively. (b) Void density through the sample length taken in the radial direction with the origin at the inner surface. (c) Size distribution of the non-coalesced voids in P91 and E911 steels. The solid line is the fit of size distribution of the creep cavities based on the expression derived by Reidel on the basis of nucleation and growth of the voids.[118]

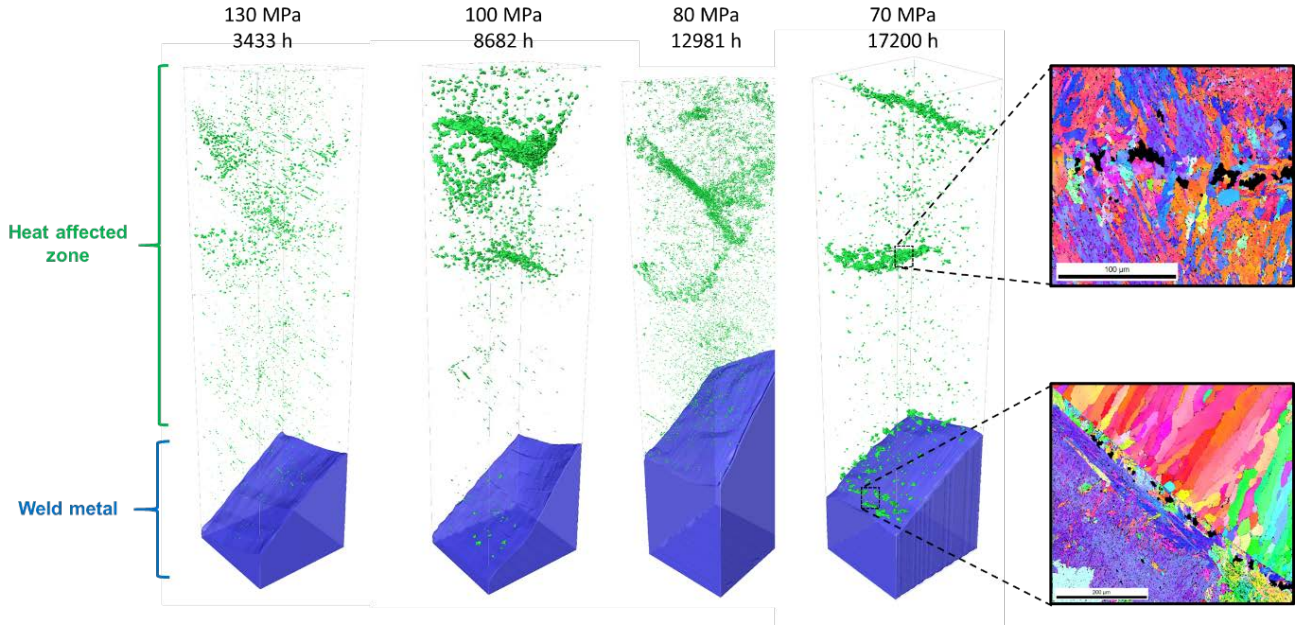

Fig. 17 3D visualisation of the volume subjected to tomography scanning of coupons extrcated from the creep tested crossweld specimen subjected to creep over the stress range 70 – 130 MPa. EBSD maps of local regions within the scanned volume are also shown[121].